

1,2,3-Triazole Tethered Hybrid Capsaicinoids as Antiproliferative Agents Active against Lung Cancer Cells (A549)

Arif Khan, Fatima Naaz, Rafia Basit, Deepak Das, Piyush Bisht, Majeed Shaikh, Bilal Ahmad Lone, Yuba Raj Pokharel, Qazi Naveed Ahmed, Shazia Parveen, Intzar Ali, Shashank Kumar Singh, Gousia Chashoo,* and Syed Shafi*



Cite This: *ACS Omega* 2022, 7, 32078–32100



Read Online

ACCESS |



Metrics & More

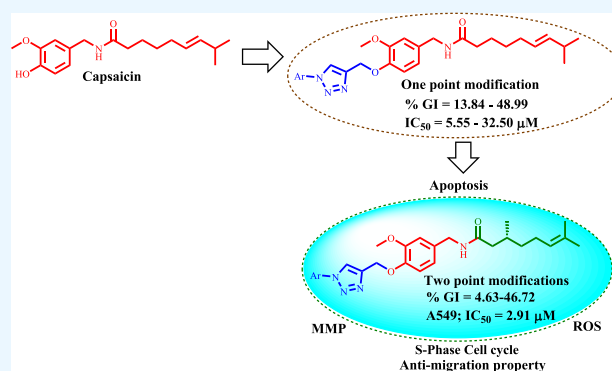


Article Recommendations



Supporting Information

ABSTRACT: A series of novel 1,2,3-triazole derivatives of capsaicin and its structural isomer (new natural product hybrid capsaicinoid) were synthesized by exploiting one-/two-point modification of capsaicin without altering the amide linkage (neck). The newly synthesized compounds were screened for their antiproliferative activity against an NCI panel of 60 cancer cell lines at a single dose of 10 μM . Most of the compounds have demonstrated reduced growth between 55 and 95%, whereas capsaicin (**10**) has shown reduced growth between 0 and 24%. Compounds showing more than 50% growth inhibition were further evaluated for the IC_{50} value. Among the cell lines tested, lung cancer cell lines (A549, NCI-H460) were found to be more susceptible toward most of the synthesized compounds. Compounds **14g** and **14j** demonstrated good anti-proliferative activity in NCI-H460 with IC_{50} values of 6.65 and 5.55 μM , respectively, while compounds **18b**, **18c**, **18f**, and **18m** demonstrated potential antiproliferative activity in A549 cell lines with IC_{50} values ranging between 2.9 and 10.5 μM . Among the compounds, compound **18f** was found to demonstrate the best activity with an IC_{50} value of 2.91 μM against A549. Furthermore, **18f** induces cell cycle arrest at the S-phase and disrupts the mitochondrial membrane potential, reducing cell migration potential by inducing cellular apoptosis and higher ROS generation along with a decrease in mitochondrial membrane potential in addition to surface and nuclear morphological alterations such as a reduction in the number and shrinkage of cells coupled with nuclear blabbing indicating the sign of apoptosis of A549 non-small cell lung cancer cell lines. Compound **18f** has emerged as a lead molecule and may serve as a template for further discovery of capsaicinoid scaffolds.



products have gained a lot of interest in cancer drug discovery. More than 70% of anticancer drugs are directly derived from natural sources, developed through structural modifications, or inspired by natural products.^{10–12} Inspired by natural product scaffolds, structural modifications of natural products have evolved as a major area in drug development. A wide variety of secondary leads had emerged *via* structural modifications/semisynthetic modifications of natural products, and several of them are in the market.^{10,13}

INTRODUCTION

Despite the recent advances in therapies, cancer is still the second leading cause of death and a major cause of morbidity and mortality worldwide. Lung cancer is responsible for around 20% of all cancer deaths with an estimated 1.8 million new cases and 1.6 million deaths annually.¹ Lung cancer represents one of the most malignant tumors, and non-small cell lung cancer (NSCLC, accounts for 80–85% of lung cancer cases) is the most aggressive type of lung cancer.^{2–4} Currently, chemotherapy is the standard treatment for patients with advanced non-small cell lung cancer. The absence of effective anti-lung cancer drugs makes the mortality of lung cancer still high. The high toxicity, low tumor specificity, and increasing resistance to available chemotherapeutic agents^{5,6} demand new drug candidates with high activity and efficacy against lung cancer.^{7–9}

Due to the invasiveness, toxicity, and ineffectiveness of current therapeutic approaches, there has been renewed interest in using natural-product-based compounds for the treatment of cancer. Over the past few decades, natural

Capsaicin (**10**) is a major spicy component of chili peppers that are consumed as spices in many cultures worldwide. It has been used medicinally for centuries and is known for its analgesic,^{14,15} antioxidant,¹⁶ chemopreventive,¹⁷ chemothera-

Received: May 28, 2022

Accepted: August 15, 2022

Published: September 1, 2022



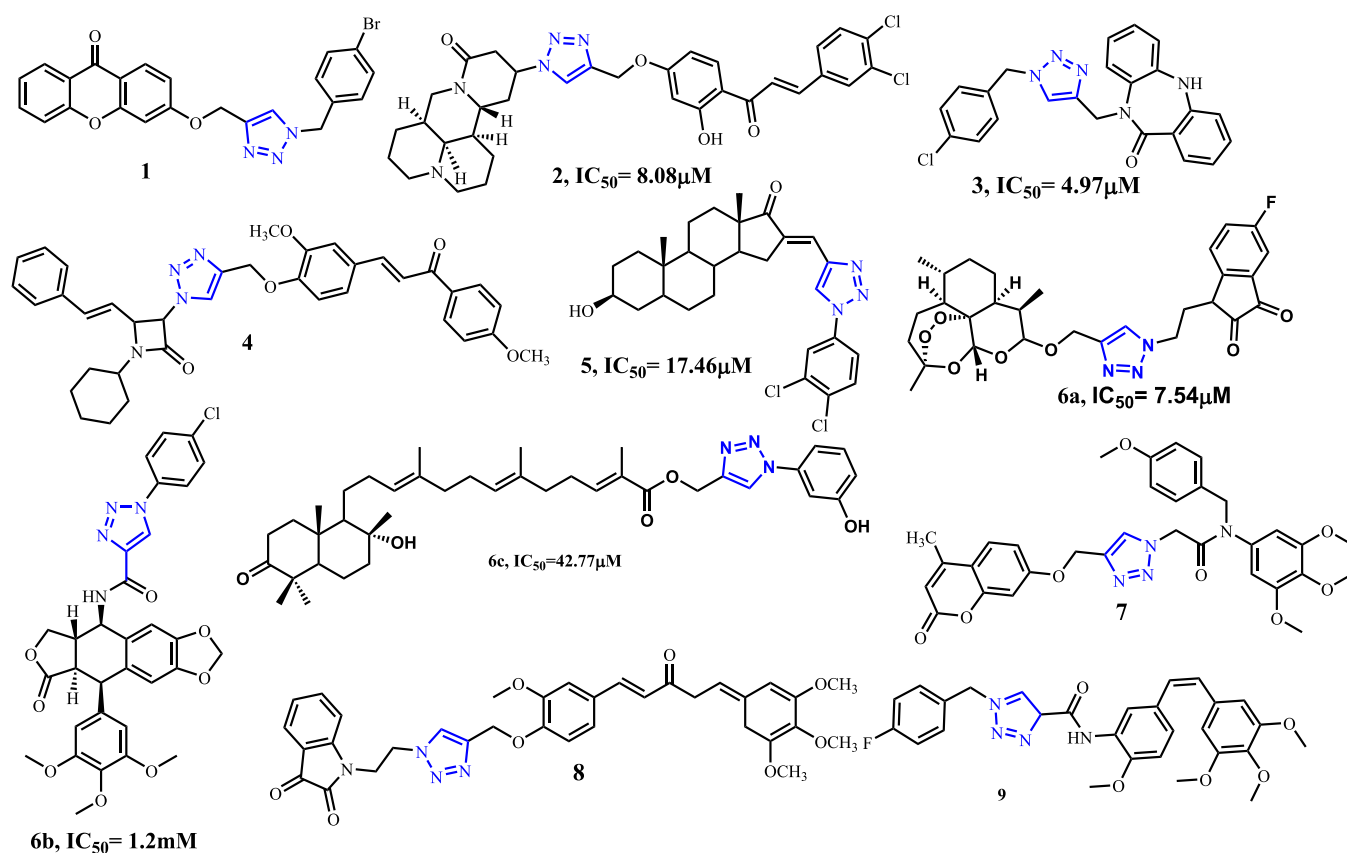


Figure 1. Rational for designing novel analogues embedded with 1,2,3-triazoles.

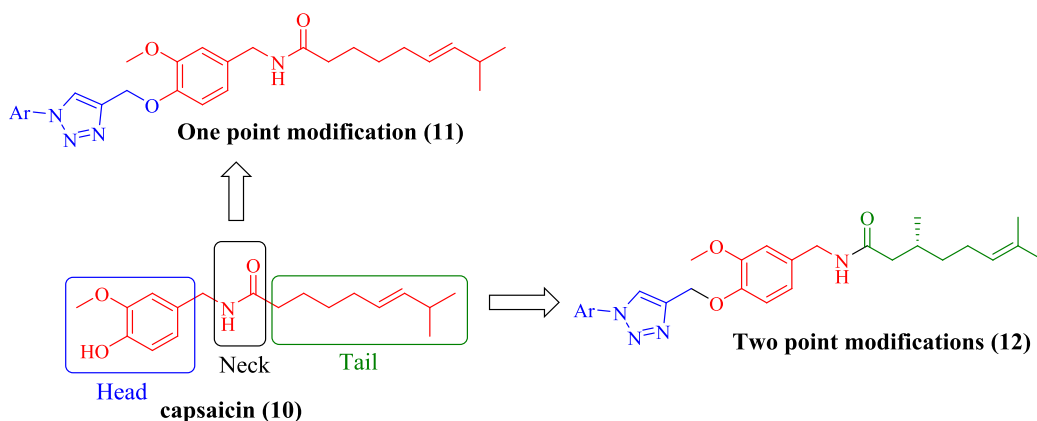
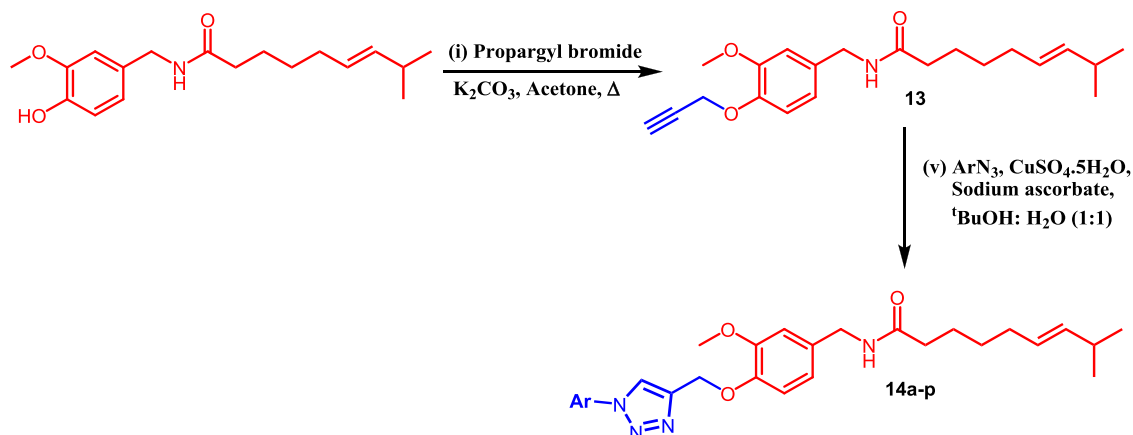


Figure 2. 1,2,3-Triazole tethered capsaicinoids through one-/two-point modifications.

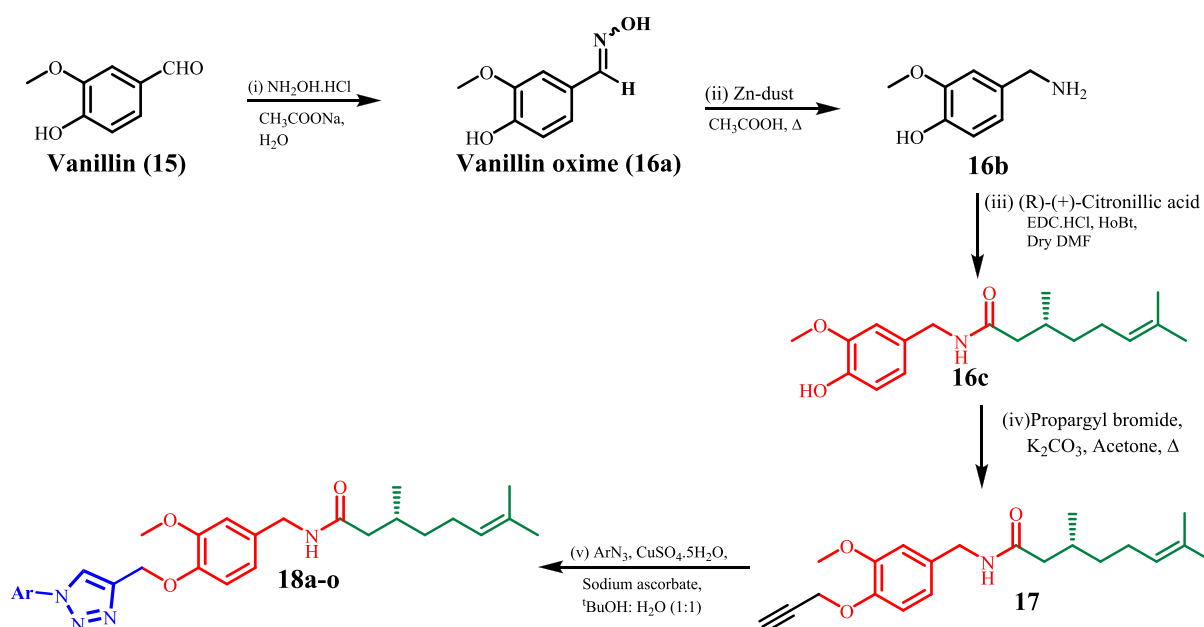
peptic,¹⁸ antidiabetic,¹⁹ anti-inflammatory,²⁰ and antiobesity²¹ properties. Capsaicin and its derivatives were also found to be potent inhibitors of bacterial (*Staphylococcus aureus* SA-1199B) NorA efflux pumps.²² Capsaicin has demonstrated *in vitro* and *in vivo* anticancer activity against a variety of cancer types.^{23–25} Studies also revealed that capsaicin may act as a carcinogen or co-carcinogen.^{26,27} One of the broadly believed mechanisms is the interaction of capsaicin with transient receptor potential vanilloids (TRPVs). TRPVs lead to Ca^{2+} -mediated mitochondrial damage and release cytochrome *c* that ultimately causes the cell apoptosis. It was found to be a robust apoptotic agent, but the low activity profile, toxicity at higher doses, and pungent nature limit its use as an anticancer agent.^{16,23} Capsaicin is approved as a topical treatment of neuropathic pain. Capsaicin selectively activates TRPV1, a Ca^{2+} -permeable

cationic ion channel that is enriched in the terminals of selected nociceptors. The limited analgesic potential for the use of systemically administered capsaicin studies in animals using local or topical application has yielded conflicting results. However, the side effects caused by capsaicin including pungency, rise in blood pressure, itching, musculoskeletal disorder, hyperalgesia, fatigue, vomiting, transient hypertension, stinging, and erythema at the application site limit its application as an oral therapeutic agent.^{28–30} Capsaicin, which inhibits VEGF, should be a key component in the development of novel anticancer therapies for NSCLC remission. Endothelial cells express VEGFR-2 (tyrosine kinase receptor), which is an effective target for suppressing tumor cell proliferation and metastasis, and it plays a crucial role in antiangiogenesis.^{23,31–33}

Scheme 1. Synthesis of 1,2,3-Triazole Tethered Capsaicin Derivatives



Scheme 2. Synthesis of 1,2,3-Triazole Tethered Natural Product Hybrid Capsaicinoids



On the other hand, the 1,2,3-triazole moiety is a key pharmacophore exhibiting a wide range of pharmacological activities.^{22,34–39} The 1,2,3-triazole moiety plays a significant role in medicinal chemistry owing to its capability of forming a hydrogen bond, which improves its solubility and ability to favorably interact with bimolecular targets.^{40–42} 1,2,3-Triazoles are highly stable to metabolic degradation as compared to other heterocyclic compounds.^{43–45} Several 1,2,3-triazole tethered natural product scaffolds like oleanolic acid,⁴⁶ quinolone,⁴⁷ isatin,⁴⁷ myrrhanone C,⁴⁸ podophyllotoxin,⁴⁹ artemisinin,³ coumarin,⁵⁰ and curcumin⁵¹ with a hydrophobic character have demonstrated potential antiproliferative activities against lung cancer cell lines (Figure 1). Conjugation of the 1,2,3-triazole moiety evidenced to be one of the important strategies to improve the anticancer properties of natural scaffolds, and many secondary leads have been developed by this approach.

The anticancer properties of capsaicin as a robust apoptotic inducing agent and the long hydrophobic side chain present in capsaicin make it an ideal scaffold for the development of secondary leads against lung cancer.^{5,6,52,53} In view of the low

anticancer activity profiles of capsaicin and the biological importance of the 1,2,3-triazole moiety toward the development of anticancer secondary leads against lung cancer, we aim to develop some new 1,2,3-triazole conjugates of capsaicin through one-/two-point modification of capsaicin as shown below (Figure 2).

RESULTS AND DISCUSSION

Chemistry. The designer molecules were synthesized through one-/two-point modification of capsaicin by employing a multistep synthetic strategy starting from vanillin as shown in Schemes 1 and 2. The one-point modification was carried at the vanillyl group (head) of capsaicin, while the two-point modification was carried out by varying the lipid group (tail) and vanillyl group (head).

One-Point Modification. Natural capsaicin (10) was treated with propargyl bromide to give the propargylated intermediate (13). Finally, the propargylated intermediate was reacted with different substituted aromatic azides under Cu-I catalyzed click chemistry conditions to afford the desired molecules (14a–p) bearing the 1,2,3-triazole moiety (Scheme 1). All the

Table 1. Chemical Structure of the Synthesized Compounds (18a–o)

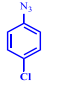
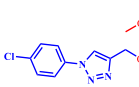
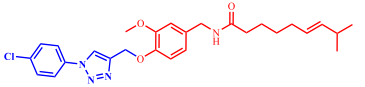
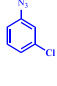
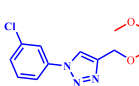
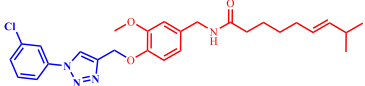
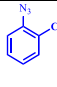
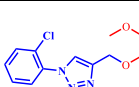
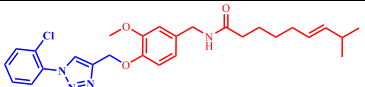
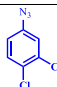
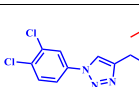
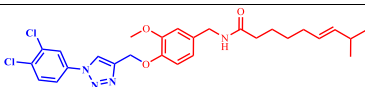
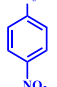
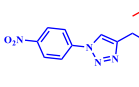
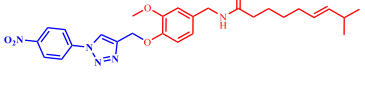
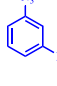
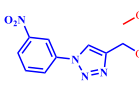
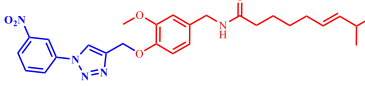
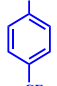
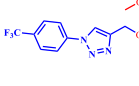
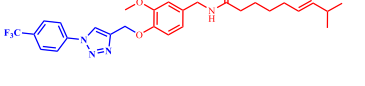
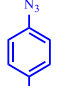
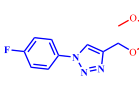
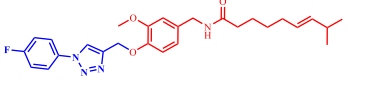
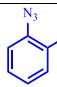
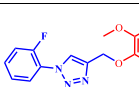
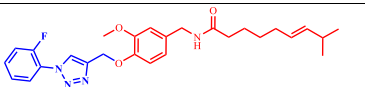
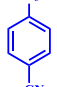
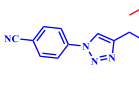
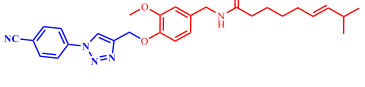
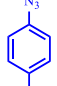
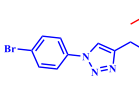
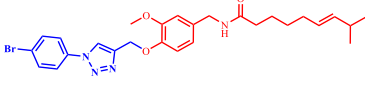
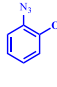
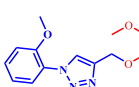
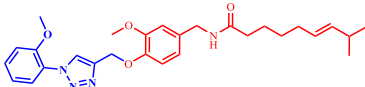
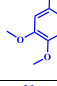
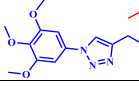
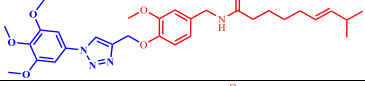
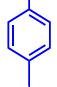
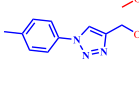
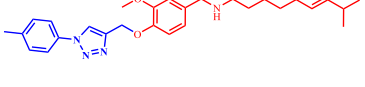
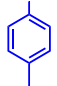
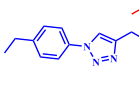
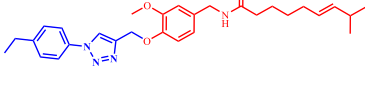
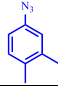
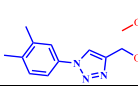
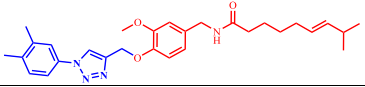
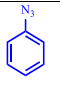
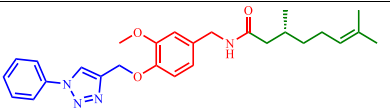
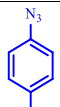
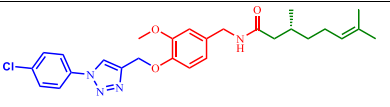
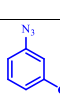
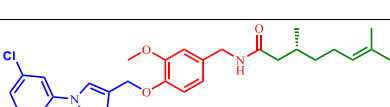
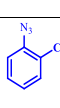
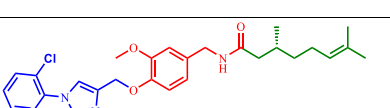
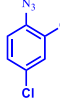
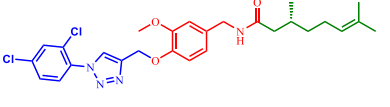
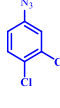
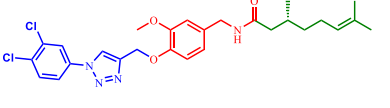
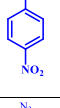
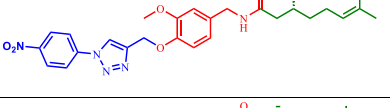
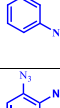
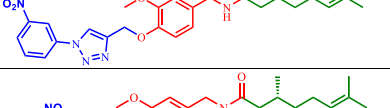
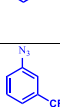
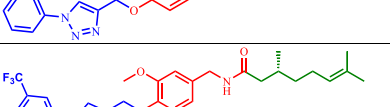
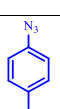
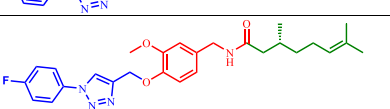
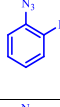
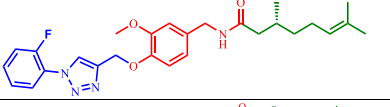
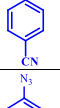
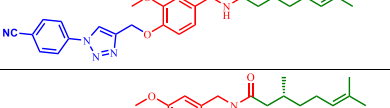
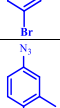
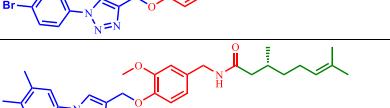



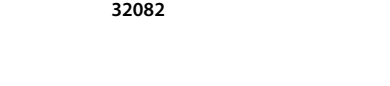
Sr No	Azides	Structure	Product	% Yield	M.P. (°C)
14a				94.0	130.2
14b				87.0	135.0
14c				98.0	88.6
14d				91.0	131.1
14e				95.0	131.0
14f				93.0	164.7
14g				89.0	156.3
14h				95.0	118.0
14i				93.0	113.0
14j				84.0	178.3
14k				91.0	127.8
14l				97.0	112.6
14m				89.0	106.2
14n				94.0	115.4
14o				90.0	105.1
14p				97.0	109.1

Table 2. Chemical Structure of the Synthesized Natural Product Hybrid Compounds (18a–o)

Sr No	Structure		% Yied	MP °C
	Azides	Product		
18a			71.2	113.2
18b			77.5	132.5
18c			85.1	162.3
18d			76.3	102.1
18e			76.3	141.3
18f			74.7	152.5
18g			83.1	151.0
18h			89.4	154.1
18i			91.7	86.1
18j			81.8	162.3
18k			71.4	132.5
18l			80.0	119.1
18m			76.4	140.0
18n			74.0	154.7
18o			91.1	91.3

synthesized compounds (**14a–p**) with their melting point are illustrated in Table 1.

Formation of propargylated capsaicin (**13**) was confirmed by the disappearance of a singlet corresponding to the phenolic –OH peak of capsaicin (**10**) at δ 8.83 ppm and the appearance of a doublet corresponding to –CH₂– at δ 4.73 ppm and a singlet corresponding to alkynyl –CH (terminal alkyne) at δ 3.53 ppm in ¹H NMR. Formation of 1,4-disubstituted 1,2,3-triazole derivatives (**14a–p**) through 1,3-dipolar cycloaddition between propargylated capsaicin (**13**) and aryl azides was confirmed by the presence of a singlet corresponding to the triazolyl proton in the range of δ 8.06–8.63 ppm, disappearance of the signal corresponding to alkynyl –CH at δ 3.53 ppm, and presence of an additional aromatic signal in ¹H NMR. The appearance of signals corresponding to triazolyl and aromatic carbons in addition to the capsaicin signals⁵⁴ in ¹³C NMR spectra further confirms the formation of target molecules. Finally, the formation of all the target molecules was confirmed by mass spectra.

Two-Point Modification. Vanillin (**15**) was reacted with hydroxylamine hydrochloride in the presence of sodium acetate trihydrate to afford the corresponding oxime (**16a**). The oxime (**16a**) was reduced to the corresponding benzyl amine (**16b**) by using Zn/CH₃COOH. 3-Methoxy-4-hydroxy benzylamine was coupled with *R*-(+)-citronellic acid to afford the hybrid natural product conjugate under EDC-HCl coupling conditions. The natural product hybrid (**16c**) was further reacted with propargyl bromide to yield the propargylated intermediate (**17**). This propargylated intermediate was finally reacted with different substituted aromatic azides under Cu-I catalyzed click chemistry conditions to afford the new target molecules (**18a–o**) bearing the 1,2,3-triazole moiety (Scheme 2). All the synthesized compounds with their melting point are illustrated in Table 2.

Formation of vanillin oxime (**16a**) from vanillin was defined by the presence of a broad doublet corresponding to one proton at 7.75–7.71 ppm (–N–OH) and 5.90 ppm (–OH). Reduction of oxime to benzylamine (**16b**) was confirmed by the absence of peaks corresponding to aldoxime at 7.75 and 5.90 ppm and the presence of a triplet at δ 3.64–3.67 ppm corresponding to two protons (–CH₂). Formation of amide (**16c**) from vanillyl amine and *R*-(+)-citronellic acid was confirmed by the appearance of two triplets at 5.47 and 5.07 ppm corresponding to an –NH of amide and an olefinic proton (HC=C) and other signals at the aliphatic region corresponding to *R*-(+)-citronellic acid. Propargylation of **16c** to **17** was recognized by the presence of a triplet at δ 2.50 ppm corresponding to terminal alkyne and the presence of additional –CH₂ protons at δ 4.73 ppm. Finally, formation of 1,2,3-triazoles (**18a–o**) from the propargylated intermediate (**17**) was affirmed by the presence of a singlet at δ 8.06–8.18 ppm (CDCl₃, ¹H NMR) corresponding to the –CH– proton of the 1,2,3-triazole moiety and the absence of signal at δ 2.50 ppm. Finally, formation of the compounds was confirmed by ¹H NMR, ¹³C NMR, LC–MS, and HR–MS.

Biology. Antiproliferative Investigation against 60 Cell Lines. Newly synthesized 1,2,3-triazole conjugates of capsaicin (**14a–p**) and 1,2,3-triazole conjugates of the structural isomer of capsaicin (**18a–n**) were submitted to the Developmental Therapeutic Program-National Cancer Institute, Bethesda, USA (www.dtp.nci.nih.gov). These synthesized compounds were selected for the screening at a single dose of 10 μ M and

tested against 60 cancer cell lines under nine different cancer cell types (leukemia, lung, colon, CNS, melanoma, ovarian, renal, prostate, and breast cancers) with their subpanels. Screening results of *in vitro* antiproliferative activity of the tested compounds were reported as growth percent as shown in Tables 3 and 4. Compounds **18a**, **18c**, **18h**, **18k**, and **18o** were screened against a panel of five human cancer cell lines, *viz.*, breast (MCF-7), colon (HCT-116), lung (A549), pancreas (MiaPaCa), and prostate (PC-3) at 10 μ M concentration, and the results are reported in percentage growth inhibition (GI) as depicted in Table 5.

Among the capsaicin derivatives (**14a–p**), compounds **14f**, **14p**, **14j**, **14g**, and **14k** illustrated susceptibility against the HCT-116 colon cancer cell line with 2.97–49.09% growth of cancer cell. Compound **14g** demonstrated better antiproliferative activity against HOP-92, NCI-H460, HCT-116, 786-0, and SN12C cancer cell lined with growth of 2.97–20.45%. It also exhibited moderate antiproliferative activity with growth of 41.33–49.67% against A549/ATCC non-small cell lung cancer, SW-620 colon cancer, SNB-75 CNS cancer, U251 CNS cancer, OVCAR-5 ovarian cancer, and OVCAR-8 ovarian cancer cell lines. Herein, compounds **14e** and **14j** displayed potent activity against NCI/ADR-RES ovarian cancer and HCT-116 colon cancer with 28.98 and 15.41% growth, respectively. Compound **14j** also demonstrated moderate antiproliferative activity against prostate PC-3 cancer cell line with a growth of 44.39%. Potent compounds (**14g**, **14j**) that showed excellent activity from the preliminary screening (NCI antiproliferative data) were further evaluated for their IC₅₀ values.

Inspired by the potent antiproliferative activity of 1,2,3-triazole tethered capsaicinoids, a series of (**18a–o**) 1,2,3-triazole derivatives of the structural isomer of capsaicin, which was derived by the hybrid conjugate of vanillyl amine and citronellic acid, were prepared and evaluated for their antiproliferative activity. Antiproliferative data revealed that compounds **18a–n** exhibited cytotoxicity against various cancer cell lines. Compound **18b** exhibited excellent activity against HCT-116, SNB-75, OVCAR-8, NCI/ADR-RES, ACHN, CAKI-1, and MDA-MB-468 with a range of growth of 38.23–49.14%. Compound **18d** showed excellent activity against leukemia (CCRF-CEM, HL-60(TB), K-562, MOLT-4, RPMI-8226, SR), HCT-116, SK-MEL-5, UACC-62, OVCAR-4, OVCAR-8, NCI/ADR-RES, CAKI-1, UO-31, PC-3, MCF-7, BT-549, T-47D, and MDA-MB-468 with a growth range of 5.29–49.81%. Moreover, compound **18e** also displayed moderate cytotoxicity against the non-small cell lung cancer HOP-62 cell line; CNS cancer SF-295, SNB-19, and SNB-75 cell lines; ovarian cancer OVCAR-4, OVCAR-8, NCI/ADR-RES, and SK-OV-3 cell lines; renal cancer CAKI-1 and RXF 393; and breast cancer HS 578T cell line with a growth range of 7.99–49.98%. Compound **18f** exhibited moderate activity against SR, A549, NCI-H460, HCT-116, HCT-15, SW-620, SF-539, SNB-75, U251, OVCAR-8, NCI/ADR-RES, SN12C, MCF7, and T-47D cancer cell lines with a growth range of 5.30–49.58%. Compound **18g** also exhibited good activity against SR, NCI-H23, HCT-116, SF-539, SK-MEL-28, NCI/ADR-RES, UO-31, T-47D, and MDA-MB-468 cancer cell lines with a growth range of 17.58–46.14%. Compound **18h** has demonstrated promising activity against NCI/ADR-RES cell lines with a growth of 3.67%. Among all other synthesized compounds, only compound **18i** demonstrated moderate activity against the leukemia (CCRF-CEM, HL-60(TB), K-

Table 3. Antiproliferative Activity of Synthesized 1,2,3-Triazole Tethered Capsaicin (14a–p) against an NCI Panel of 60 Human Cancer Cell Lines

cancer panel	subpanel/comp no.	14a	14b	14c	14d	14e	14f	14g	14h	14i	14j	14k	14l	14m	14n	14o	14p
leukemia	CCRF-CEM	72.44	87.33	87.87	84.65	84.94	90.24	68.85	79.73	88.58	86.21	94.23	83.65	96.33	87.34	86.83	75.54
	K-562	66.66	84.87	76.84	77.13	74.53	81.49	76.27	68.74	82.35	75.37	59.18	76.13	79.71	79.98	78.64	74.64
	MOLT-4	81.99	92.80	81.04	86.41	79.33	86.56	80.34	82.62	90.94	88.39	77.45	79.70	92.05	83.54	79.62	78.54
	RPMI-8226	60.83	86.29	75.55	78.11	61.80	65.86	53.37	68.40	81.34	65.44	57.35	71.25	79.37	74.10	73.95	67.31
	SR	73.55	85.61	68.45	78.92	62.18	78.38	70.36	76.67	81.54	76.32	67.19	77.40	86.62	75.55	87.52	58.25
non-small cell lung cancer	A549/ATCC	85.32	82.93	84.33	85.90	84.06	91.99	48.99	84.35	91.27	84.82	88.49	85.96	91.04	84.04	88.34	82.16
	EKVX	72.02	80.81	82.11	76.21	75.28	95.11	88.25	72.71	79.11	90.82	72.66	89.40	95.93	84.83	82.11	79.28
	HOP-62	83.97	71.45	81.95	90.38	80.87	97.38	64.56	84.07	88.21	102.9	88.21	88.73	90.68	86.39	94.51	97.43
	HOP-92	77.10	62.44	80.14	78.72	80.32	70.38	13.84	66.16	78.66	80.48	68.79	72.06	82.53	83.54	86.50	80.41
	NCI-H226	70.36	86.45	81.77	76.64	89.59	90.88	53.63	74.15	81.34	100.5	86.31	80.50	91.44	75.82	76.71	86.88
colon cancer	NCI-H23	78.67	87.17	93.56	93.19	83.21	87.96	94.56	81.41	95.32	72.14	70.17	96.02	90.08	87.91	89.51	74.91
	NCI-H322M	92.15	86.20	89.36	93.25	97.91	94.09	96.15	91.76	90.16	95.29	90.64	92.18	89.07	89.39	90.50	101.0
	NCI-H460	79.92	84.09	101.3	101	99.76	91.79	16.74	75.71	103.5	92.96	72.09	104.4	101.5	93.21	102.7	86.45
	NCI-H522	65.69	69.17	64.46	69.27	78.21	82.60	75.57	70.15	77.48	88.19	82.50	63.91	65.21	62.09	65.93	80.70
	COLO205	108.5	102.4	106.4	110.6	117.9	106.8	72.59	119.9	115.7	117.3	103.1	116.8	106.2	115.2	120.9	106.5
CNS cancer	HCC-2998	112.7	104	110.5	98.1	107.5	101.2	94.75	110.2	97.17	94.51	88.79	117.3	91.82	108.4	99.66	100.6
	HCT-116	63.68	76.84	100.3	106.8	77.19	41.96	2.97	65.61	97.81	15.41	49.09	82.68	87.14	92.44	90.69	48.16
	HCT-15	91.77	91.31	94.11	93.61	96.24	77.90	59.70	89.61	95.97	83.47	94.02	106.1	103.2	103.9	94.42	71.18
	HT29	88.41	99.25	98.23	99.43	98.13	88.86	78.99	106.0	106.9	95.56	98.09	98.69	87.19	100.1	109.4	97.85
	KM12	95.56	98.56	97.72	99.98	90.03	91.20	81.18	94.49	98.88	91.46	94.30	98.21	102.6	96.05	100.3	97.54
melanoma	SW-620	88.74	92.82	100.1	96.12	97.40	97.40	41.33	90.98	98.10	98.02	94.70	96.98	102.4	102.4	102.7	95.17
	SF-268	84.04	82.49	87.78	93.32	86.10	92.25	87.80	87.23	95.04	90.86	78.89	92.64	90.52	81.74	93.05	94.60
	SF-295	88.30	90.53	99.41	94.64	89.02	103.9	90.90	90.52	98.96	102.1	85.39	107.6	105.4	98.90	100.05	88.82
	SF-539	87.11	81.97	104.2	96.14	104.1	94.44	81.86	92.18	104.8	94.55	92.40	106.3	92.01	100.3	103.68	105.0
	SNB-19	87.72	59.97	89.74	87.31	97.39	68.23	76.10	81.35	84.84	81.91	80.91	91.56	85.13	77.94	85.68	95.85
ovarian cancer	SNB-75	76.44	75.84	87.34	79.08	83.94	91.95	49.67	83.46	88.08	94.17	90.92	103.3	95.25	99.45	92.63	90.98
	U251	86.89	69.08	85.65	91.90	86.36	85.29	46.69	83.87	93.12	91.16	75.48	90.23	92.80	81.65	89.37	88.35
	LOX IMVI	85.61	89.42	89.93	87.04	89.50	92.87	60.32	84.23	87.12	78.15	83.68	86.08	94.42	85.10	89.32	84.46
	MALME-3M	97.85	98.65	107.4	105.3	98.44	103.1	99.71	103.2	107.7	102.3	102.7	106.2	98.49	109.8	107.95	107.2
	M14	90.64	94.14	92.57	92.67	89.72	93.4	97.51	94.05	96.85	95.27	90.17	96.66	94.53	93.33	99.82	93.54
ovarian cancer	MDA-MB-435	99.29	98.61	102.6	94.22	99.74	101.2	107.0	98.80	100.6	107.7	106.9	109.6	106.5	109.0	107.0	104.3
	SK-MEL-2	101.6	86.66	90.98	108.4	91.96	88.40	95.06	111.3	105.5	98.43	95.21	89.80	97.57	91.94	95.17	90.32
	SK-MEL-28	106.5	105.7	105.8	104.0	102.4	105.9	107.0	102.5	107.3	104.6	100.4	115.6	108.1	113.7	114.9	112.1
	SK-MEL-5	77.63	91.17	89.83	81.64	76.10	93.24	97.06	83.73	91.50	86.97	72.04	83.94	77.50	86.78	83.95	81.53
	UACC-257	91.64	90.11	87.93	89.23	82.58	94.42	98.24	90.21	94.96	94.35	90.46	85.25	93.58	88.19	86.37	81.89
ovarian cancer	UACC-62	67.84	74.98	73.31	75.61	69.29	70.05	84.33	71.93	76.23	81.83	62.99	75.07	87.79	70.18	71.39	75.07
	IGROV1	93.44	79.91	98.76	104.1	90.41	89.40	58.71	96.98	100.8	100.4	72.65	104.5	103.3	98.46	102.5	98.81
	OVCAR-3	104.9	84.40	101.1	92.4	92.69	104.9	106.8	96.37	97.52	108.9	100.1	103	103.1	91.85	101.0	100.4
	OVCAR-4	82.64	67.25	87.87	69.52	87.18	94.19	98.59	82.15	84.19	94.94	89.23	99.97	103.4	88.79	88.97	84.94
	OVCAR-5	100	99.78	103.5	102.4	99.15	107.3	96.56	97.57	102.6	95.30	116.2	112.8	109.1	108.4	112.13	107.4
ovarian cancer	OVCAR-8	78.97	57.20	89.57	91.05	82.87	76.93	41.06	71.55	94.5	63.28	79.60	82.16	88.18	76.53	91.14	83.35
	NCI/ADR-RES	78.12	76.59	92.04	91.11	28.98	81.79	48.24	70.62	89.77	79.67	71.97	94.61	91.69	87.43	87.71	80.64
	SK-OV-3	91.64	78.80	91.28	97.24	76.69	93.55	91.30	86.36	97.84	88.22	74.85	99.76	89.94	94.38	101.6	98.61

Table 3. continued

cancer panel	subpanel/comp no.	14a	14b	14c	14d	14e	14f	14g	14h	14i	14j	14k	14l	14m	14n	14o	14p
renal cancer	786-0	92.52	76.84	93.81	96.31	93.73	73.38	2.94	83.74	97.19	91.65	92.05	102.4	107.6	99.62	100.2	99.82
	ACHN	59.66	72.99	74.08	58.30	81.98	78.92	85.84	81.18	82.95	74.59	87.69	79.93	79.48	72.01	77.39	68.45
	CAKI-1	88.99	79.62	93.42	100.6	90.66	81.67	90.23	88.42	90.63	90.77	74.31	101.0	104.4	88.54	101.0	94.35
	RXF 393	97.98	91	104.9	100.6	99.73	92.69	90.23	95.34	103.1	90.77	105.4	101.0	104.4	102.5	101.0	98.20
prostate cancer	SN12C	80.18	84.24	94.47	112.6	91.67	89.51	65.57	82.38	92.65	98.27	83.0	98.02	101.6	89.3	98.54	88.40
	TK-10	99.28	105.5	94.57	88.62	92.72	104.9	20.45	103.0	111.3	91.84	117.5	90.25	91.59	100.6	87.44	108.97
	UO-31	76.58	72.21	75.19	102.7	60.63	74.73	92.75	86.04	77.11	111.8	67.93	105.0	116.9	75.81	93.93	75.67
	PC-3	79.23	83.59	80.60	70.08	77.97	82.16	70.50	84.14	82.05	79.46	73.69	73.46	80.91	84.17	70.87	78.43
breast cancer	DU-145	98.92	95.88	99.19	86.53	104.7	108.7	62.20	96.08	105.8	44.39	98.83	83.12	85.40	96.95	93.77	107.95
	MCF-7	84.88	86.88	97.24	95.33	83.45	74.06	80.73	89.31	97.12	103.0	76.17	98.16	102.3	96.29	102.2	86.88
	MDA-MB-231 ATCC	79.50	64.80	80.85	87.29	75.32	88.39	75.16	69.06	78.71	90.83	71.32	95.76	92.66	72.21	88.05	89.27
	HS 578T	90.35	74.80	97.20	84.04	95.78	90.76	70.69	77.70	87.70	95.03	90.48	83	69.00	89.68	78.03	90.74
	BT-549	86.83	99.35	90.81	91.78	80.40	96.27	80.41	91.05	89.25	91.24	88.08	93.12	79.12	105.0	99.09	93.65
	T-47D	71.04	81.08	74.30	87.05	63.99	72.34	84.51	73.75	83.08	76.82	68.37	92.18	95.75	77.41	111.0	73.17
	MDA-MB-468	64.91	74.73	88.19	71.60	77.44	72.34	70.22	68.19	92.81	74.86	68.15	75.45	80.43	92.44	79.80	71.77

562, MOLT-4, RPMI-8226, SR), colon cancer (HCT-116, HT29), melanoma (SK-MEL-5, UACC-62), ovarian cell (OVCAR-4, OVCAR-8, NCI/ADR-RES), renal cell (CAKI-1, UO-31), prostate cancer (PC-3), and breast cancer (BT-549, T-47D, MDA-MB-468) cell lines with a growth range of 14.05–48.65%. Compound **18f** also showed good activity against SR, A549, NCI-H460, HCT-116, SW-620, SF-539, OVCAR-4, OVCAR-8, NCI/ADR-RES, SN12C, and T-47D cancer cell lines with a growth range of 10.58–45.13%. Compounds **18l**, **18m**, and **18n** also showed good activity against K-562, MOLT-4, SR, A549, HOP-92, NCI-H460, NCI-H522, HCT-116, SNB-75, SF-295, SF-539, SNB-75, SK-OK-3, SK-MEL-5, OVCAR-4, OVCAR-8, NCI/ADR-RES, CAKI-1, 786-0, RXF 393, MCF7, HS 578T, T-47D, and MDA-MB-468 cancer cell lines with a growth range of 4.63–49.34%. Antiproliferative data revealed that compounds **18c** and **18f** exhibited excellent cytotoxicity against the lung (A549) cell line with a range of growth inhibition of 55–91%. Compound **18m** showed moderate activity against breast (MCF-7) and lung (A549) cell lines with a growth inhibition range of 51–62% (Table 4).

Determination of IC₅₀ Values. Compounds (**14g**, **14j**, **18b**, **18c**, **18f**, **18m**) showing excellent % GI against non-small cell lung cancer (A549, NCI-H460), breast cancer (MCF-7), colon cancer (HCT-116), and ovarian cancer (SKOV-3) cell lines were further evaluated for their IC₅₀ values using an SRB assay, and the results are depicted in Table 5.

Among the cell lines tested, lung cancer cell lines NCI-H460 and A549 were found to be more susceptible against these compounds. Compounds **18b**, **18c**, **18f**, and **18m** exhibited good to moderate cytotoxicity against the A549 cancer cell line with IC₅₀ values ranging between 2.91 and 10.55 μM. Among the compounds tested, compounds **18c** and **18f** demonstrated the best antiproliferative activity against A549 with IC₅₀ values of 3.68 and 2.91 μM, respectively, while compound **14g** demonstrated moderate antiproliferative activity against NCI-H460. Compound **18m** was found to be moderately active against both MCF-7 and A549 cell lines with IC₅₀ values of 9.34 and 8.44 μM, respectively. Dose–response curve of compounds **18b**, **18c**, **18f**, **18m** doxorubicin and paclitaxel against A549 and MCF-7 cell lines is depicted in Supporting Information. The standard compounds doxorubicin and paclitaxel were screened as positive control, as shown in Table 6. Compound **18f** was further evaluated for its toxicity against normal HEK-293 cells (normal kidney cells). The IC₅₀ of compound **18f** was 116-fold higher in HEK-293 (IC₅₀ = 696 μM) as compared to A549 cells.

Structure–Activity Relationship (SAR). On the basis of the *in vitro* antiproliferative results (IC₅₀) obtained, SAR of the synthesized compounds was developed based on the nature and position of the substituent present on the aromatic ring attached to the 1,2,3-triazole ring. Triazole conjugates in both series (**14a–p** and **18a–o**) were found to be highly active when compared to the nonconjugated natural capsaicin and its structural isomer (**16c**). The lipophilic side chain of 1,2,3-triazole tethered capsaicinoids greatly influenced the antiproliferative activity. Replacing the lipophilic side chain of (*R*)-*N*-(4-hydroxy-3-methoxybenzyl)-3,7-dimethyloct-6-enamide with citronellic acid significantly enhanced the activity. Further, it has been observed that the nature of the substituents on the aromatic ring connected to the 1,2,3-triazole moiety also influenced the activity. Compounds with choro/bromo/cyano substituted aromatic moiety demonstrated better activity.

Table 4. Antiproliferative Activity of Synthesized 1,2,3-Triazole (18a–n) against an NCI Panel of 60 Human Cancer Cell Lines

PANEL/NAME	comp no.	16c	18a	18b	18c	18d	18e	18f	18g	18h	18i	18j	18k	18l	18m	18n	
leukemia	CCRF-CEM	70.56	59.43	92.94	76.55	40.10	116.05	84.49	81.06	85.57	36.52	97.09	83.96	97.30	58.35	61.14	
	HL-60(TB)	76.37	93.01	87.80	83.86	41.06	95.54	83.95	110.2	100.27	47.68	96.30	89.26	91.54	70.85	88.43	
	K-562	89.43	79.40	53.52	60.82	44.62	81.37	51.89	44.88	83.08	51.53	59.00	72.74	81.62	47.60	66.32	
	MOLT-4	83.43	54.59	71.73	47.68	16.29	84.05	68.65	64.23	80.63	20.66	84.80	67.45	74.84	14.78	69.97	
non-small cell lung cancer	RPMI-8226	84.37	37.90	75.30	56.33	47.56	90.71	77.63	73.14	73.29	39.91	89.81	75.33	81.80	58.26	69.27	
	SR	90.57	62.33	65.77	61.39	48.53	79.78	27.12	39.18	81.95	45.13	41.51	68.94	73.39	24.73	63.80	
	A549/ATCC	96.36	94.07	57.07	81.77	64.07	59.42	46.49	85.48	56.83	65.65	42.61	76.78	80.64	48.20	78.59	
	EKVX	86.35	74.29	75.34	51.21	54.00	81.06	77.24	75.25	69.05	58.81	92.14	65.19	78.32	81.03	79.03	
	HOP-62	85.81	120.28	61.55	89.31	79.25	11.33	95.67	103.84	82.74	78.10	88.76	67.99	46.72	88.63	65.10	
	HOP-92	83.48	103.88	53.02	71.92	79.43	-3.27	51.60	86.49	76.24	57.55	86.10	55.58	4.63	65.16	45.94	
	NCI-H226	100.60	79.51	63.78	54.16	59.73	66.35	50.55	80.08	73.48	56.87	72.34	51.40	73.35	54.94	70.24	
	NCI-H23	94.13	91.88	64.87	72.88	64.51	56.64	68.51	45.49	66.55	62.45	79.35	74.89	68.25	64.54	60.06	
	NCI-H322M	91.13	106.92	83.48	104.66	91.28	95.25	82.51	92.29	103.37	94.44	90.10	105.20	92.68	94.96	99.60	
	NCI-H460	103.61	97.03	65.04	88.73	78.43	75.06	45.51	78.17	62.92	84.19	14.61	79.49	89.03	45.78	74.17	
NCI-H522	86.86	85.53	62.93	67.33	51.40	55.44	61.51	58.92	80.13	61.88	83.09	66.40	57.14	63.51	41.63		
colon cancer	COLO 205	105.96	99.03	91.10	102.61	71.71	104.99	53.63	121.73	94.43	78.01	74.25	97.16	111.74	95.57	112.90	
	HCC-2998	108.39	93.30	75.87	94.66	91.88	92.47	93.52	107.31	91.41	106.48	111.05	94.86	100.56	89.49	95.80	
	HCT-116	94.11	96.71	38.23	72.22	49.66	53.13	29.82	32.09	18.65	49.09	12.49	47.86	60.15	29.43	41.92	
	HCT-15	100.88	88.04	65.29	81.43	53.84	79.57	29.35	71.79	80.93	62.42	56.79	91.65	82.81	66.16	82.35	
	HT29	103.79	99.48	79.57	97.34	76.66	82.28	82.28	108.14	100.11	22.55	96.61	102.98	97.40	77.55	94.43	
	KM12	100.37	96.04	87.72	94.27	62.97	93.06	82.66	86.78	91.32	63.85	84.99	96.37	99.29	71.66	94.59	
	SW-620	98.70	76.75	97.41	80.24	89.26	89.26	29.90	86.83	80.92	92.93	38.71	101.33	92.72	71.03	91.70	
	SF-268	77.04	92.33	95.38	85.96	82.41	52.34	58.39	88.77	73.15	78.08	83.86	69.92	58.88	71.57	71.71	
	SF-295	103.18	88.16	55.55	66.84	56.38	41.76	80.45	70.15	96.45	60.45	72.87	64.41	45.20	54.05	63.24	
	SF-539	93.56	96.00	67.72	73.07	75.23	66.88	5.30	43.12	69.79	66.99	16.35	68.43	44.60	59.74	51.16	
melanoma	SNB-19	95.32	74.44	78.63	67.87	61.27	49.98	81.31	84.82	73.39	66.43	97.17	53.11	55.68	83.59	57.66	
	SNB-75	56.78	41.60	41.60	102.61	60.00	7.99	47.20	78.02	40.06	56.57	65.15	10.58	10.58	54.57	47.32	
	U251	98.73	93.80	57.71	75.06	80.61	54.40	48.23	82.82	82.82	40.06	62.83	50.97	65.37	61.60	83.86	63.36
	LOX IMVI	92.96	92.33	59.71	75.06	56.37	80.73	50.61	62.72	71.40	62.00	80.73	81.38	76.70	72.59	74.03	
	MALME-3M	90.29	88.78	68.35	87.23	68.22	79.26	77.44	76.19	71.40	70.30	80.81	96.02	78.28	75.36	85.41	
	M14	95.93	85.67	90.80	93.39	55.87	102.02	89.03	88.83	82.48	65.91	92.12	102.20	94.79	88.23	97.23	
	MDA-MB-435	102.18	97.17	84.94	93.75	66.50	98.16	91.28	88.25	99.53	74.94	74.88	103.84	100.50	81.26	98.30	
	SK-MEL-2	101.97	91.22	83.62	95.46	53.30	71.68	93.67	64.50	95.86	66.32	110.78	84.61	78.55	79.97	78.04	
	SK-MEL-28	106.36	99.70	86.95	76.60	69.78	96.28	89.28	87.77	98.47	85.31	91.55	89.56	94.93	85.39	96.54	
	SK-MEL-5	97.72	77.37	62.77	89.51	5.29	60.43	71.91	35.89	86.20	16.33	78.75	65.24	70.80	31.05	55.65	
ovarian cancer	UACC-257	112.93	101.28	85.53	72.07	60.33	91.96	91.04	69.39	92.03	71.22	103.84	69.92	94.00	68.74	86.34	
	UACC-62	81.15	64.23	65.67	108.08	39.56	65.59	69.35	53.53	65.91	48.01	72.06	64.41	69.54	56.65	65.15	
	IGROV1	89.12	88.78	80.15	95.28	87.05	72.31	83.14	78.76	106.74	78.93	102.20	97.38	81.86	81.49	89.93	
	OVCAR-3	94.85	116.94	82.26	70.95	83.57	101.33	60.12	107.92	98.44	80.34	102.85	107.56	105.46	94.05	104.69	
	OVCAR-4	78.72	95.26	52.67	106.44	33.26	49.69	53.41	63.75	63.65	45.26	45.13	73.07	71.43	55.29	49.55	
	OVCAR-5	93.28	69.23	80.72	72.31	93.08	91.71	86.36	101.94	98.00	95.61	97.48	101.77	94.92	97.97	105.21	
	OVCAR-8	99.92	107.77	49.14	57.30	49.81	29.30	46.30	63.55	23.70	48.57	28.11	52.29	66.47	59.99	47.52	
	NCI/ADR-RES	94.46	81.94	47.96	99.18	24.02	32.86	36.55	17.58	3.67	36.03	44.05	45.40	54.77	14.02	52.06	

Table 4. continued

PANEL/NAME	comp no.	16c	18a	18b	18c	18d	18e	18f	18g	18h	18i	18j	18k	18l	18m	18n
renal cancer	SK-OV-3	97.77	47.99	72.13	75.06	82.97	26.10	99.00	80.08	95.87	68.44	88.99	85.05	43.56	82.43	64.02
	786-0		113.25	84.28	92.28	87.70	38.94	80.43	97.04	71.40	83.46	92.98	68.16	43.58	96.24	68.65
	A498	103.70	92.16	98.87	141.89	106.80	58.98	79.95	92.59	91.34	107.83	90.96	136.18	103.28	92.30	104.93
	ACHN	96.18	110.84	44.83	80.22	67.59	61.09	71.52	72.71	111.72	80.79	77.61	69.02	65.32	72.75	56.39
	CAKI-1	81.89	93.22	45.87	87.58	46.28	31.84	64.04	72.08	69.51	48.65	73.63	81.82	55.08	62.58	28.75
	RXF 393	104.03	90.76	56.13	79.87	72.64	14.13	74.78	90.59	83.02	55.93	88.27	52.33	38.41	49.41	61.80
	SN12C	82.18	98.10	67.70	79.39	69.58	64.79	38.19	70.68	96.63	73.66	27.14	80.79	76.12	77.75	71.63
	TK-10	120.42	88.46	95.63	99.80	93.11	68.70	90.74	104.96	72.43	113.60	101.93	91.77	95.83	105.47	108.92
	UO-31	60.69		62.50		30.26	60.54		60.75	42.13	36.50	75.65		71.89	50.93	62.92
	PC-3	83.21	83.14	80.17	76.26	49.41	85.05	85.05	65.91	85.51	75.72	48.11	82.47	80.20	68.16	81.39
prostate cancer	DU-145	102.58	92.07	82.81	86.56	90.12	90.48	76.78	86.40	84.49	77.90	100.88	93.09	101.70	73.70	92.71
	MCF7	97.19	80.61	51.57	63.32	40.61	67.54	49.58	63.96	74.54	50.45	56.77	77.07	66.90	42.30	60.21
	MDA-MB-231/ATCC	79.57		59.59		72.60	59.66	75.74	76.76		71.94	87.20		66.80	81.38	80.58
	HS 578T		100.24	71.37	52.51	80.95	48.38	57.02	81.99	68.23	73.67	94.33	33.70	39.51	76.00	73.79
	BT-549	95.55	83.27	87.40	66.42	28.16	83.67	71.72	72.57	77.08	24.05	92.35	79.69	70.98	58.51	93.63
	T-47D	89.01	66.00	52.46	58.60	9.14	60.21	33.60	46.14	58.91	14.63	32.42	67.90	60.60	35.97	49.34
	MDA-MB-468	99.02	66.15	41.27	43.43	28.48	50.44	54.99	41.44	56.62	31.66	64.90	64.96	57.69	30.23	46.73

Table 5. Percent GI on Breast, Colon, Lung, Pancreas, and Prostate Cell Lines

tissue cell line type	breast MCF-7	colon HCT-116	lung A549	pancreas MiaPaCa	prostate PC-3	
compounds	conc. (μM)	% GI				
18a	10	10	37	31	23	03
18b	10	34	41	55	66	28
18c	10	43	78	91	45	15
18d	10	39	26	41	12	09
18e	10	12	38	25	18	06
18f	10	32	45	71	27	28
18g	10	43	32	33	53	05
18h	10	11	15	15	23	14
18i	10	28	25	16	36	01
18j	10	04	50	42	17	21
18k	10	05	22	36	42	11
18l	10	01	23	28	27	23
18m	10	51	47	62	31	05
18n	10	42	26	36	29	18
18o	10	45	26	32	21	03
capsaicin	10	24	0.0	0.0	15	19

Table 6. IC₅₀ (μM) Profile of Active Compounds

test compound	non-small cell Lung cancer		breast cancer	colon cancer	ovarian cancer	HEK-293
	A549	NCI-H460	MCF-7	HCT-116	SKOV-3	
14g	nt	6.65	nt	8.90	10.63	nt
14j	nt	5.55	nt	10.45	32.50	nt
18b	10.554	nt	nt	nt	nt	nt
18c	3.69	nt	nt	nt	nt	nt
18f	2.91	nt	nt	nt	nt	696
18m	8.44	nt	9.35	nt	nt	nt
capsaicin	nt	30.66	nt	40.16	22.03	nt
paclitaxel	0.03 nM	nt	nt	nt	nt	nt
doxorubicin	nt	4.29	0.18 nM	57.77	25.83	nt

Chloro-substitution led to better activity when compared to other substitutions. On the basis of the position of the substitution, the activity profile has been observed as 3,4-dichloro > 3-chloro > 4-chloro > 2-chloro. On the basis of SAR, the most active compound (**18f**) has been selected for further detailed studies (Figure 3).

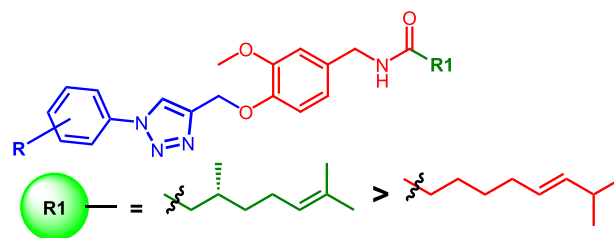


Figure 3. SAR for synthesized 1,2,3-triazoles against antiproliferative activity.

Reactive Oxygen Species (ROS) Generation Assay. A higher level of ROS generation is a prime indication of apoptosis in cancerous cells. In the current study, A549 cells were incubated with DCFDA dye, and intracellular ROS was observed using a fluorescence microscope. A higher amount of

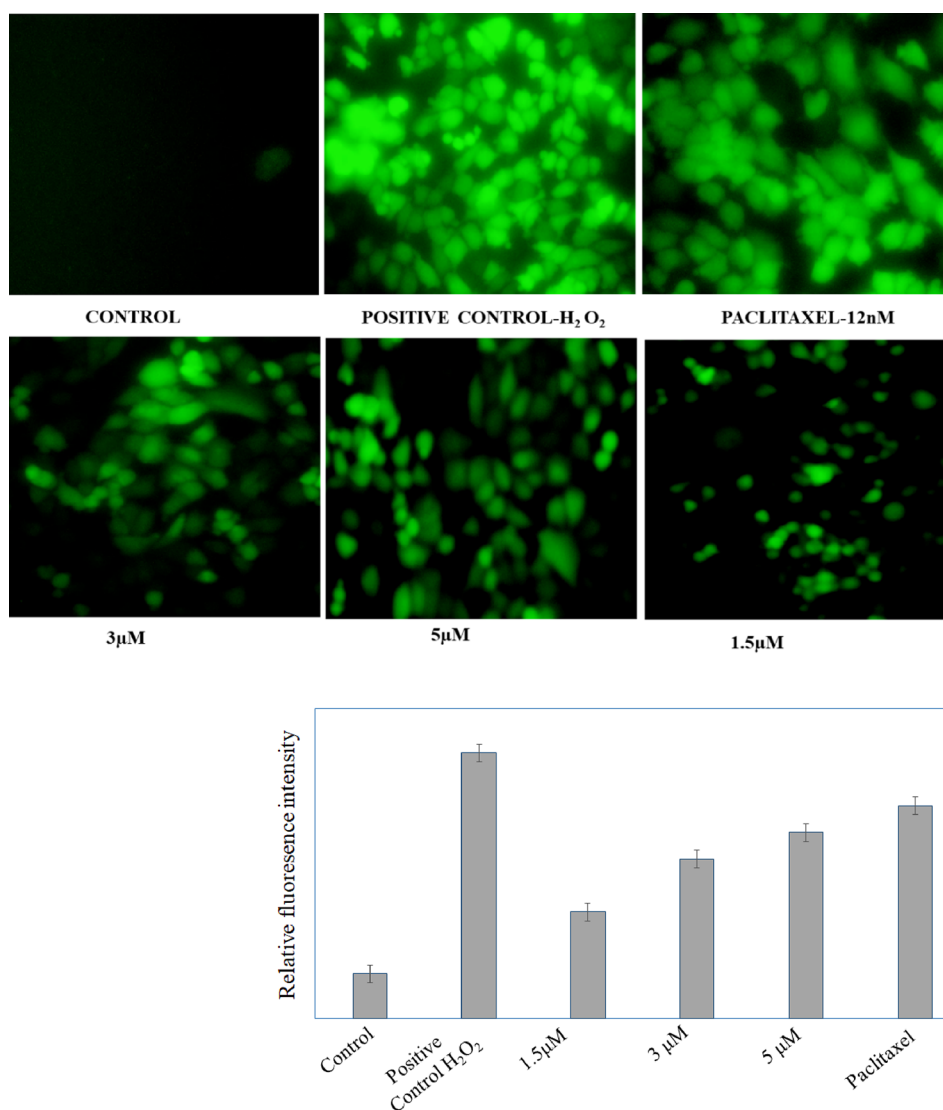


Figure 4. Determination of reactive oxygen species in A549 cells by paclitaxel and **18f**. H₂O₂ is used as positive control. Control group had no green fluorescence, and the ROS level was low in the control group but higher in the treated groups.

ROS was produced in the positive control group. In a similar way, the amount of ROS was increased after the treatment with compound **18f** at 5, 3, and 1.5 µM concentration. Observation through fluorescence microscope is a qualitative means of ROS generation in A549 lung cancer cells where a sharp increase in fluorescence intensity was observed (Figure 4). This study indicated that compound **18f** triggered ROS generation in A549 cells, which is a key feature of apoptosis.

Apoptosis Assay through DAPI Staining. DAPI staining helped differentiate between normal and apoptotic cells by the nuclear morphological changes caused in a concentration-dependent manner after treatment with compound **18f** at 5, 3, and 1.5 µM concentration against the A549 cell line. The morphological changes that have occurred can be visualized using fluorescence microscopy. The nuclei of untreated cells appeared as more or less rounded structures, while the treatment groups (**18f**) including paclitaxel showed chromatin condensation, nuclear blebbing, and formation of apoptotic bodies. The nuclear morphological changes, with the exception of the untreated control, clearly suggested that A549 cells had undergone apoptosis (Figure 5).

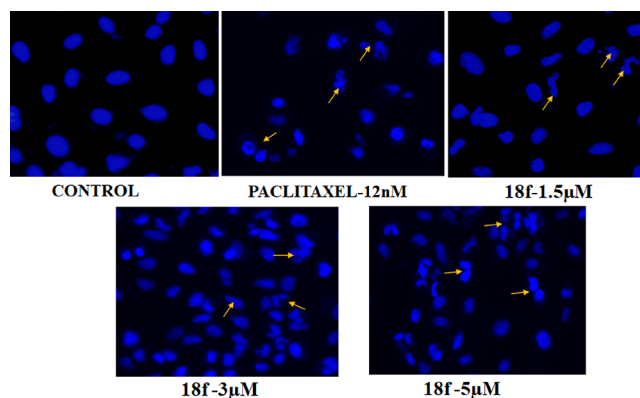


Figure 5. Fluorescence microscopy analysis of DAPI-stained cells was undertaken to study nuclear alterations and apoptotic body formation, both of which are also features of apoptosis. Effect of **18f** on nuclear morphology of A549 lung cancer cells with varying concentrations and paclitaxel as positive control was assessed after DAPI staining. Arrows represent the changes in the nuclear structure such as chromatin condensation and nuclear damage.

Measurement of Loss of Mitochondrial Membrane Potential ($\Delta\Psi_m$). Reduction of MMP ($\Delta\Psi_m$) is the main characteristic of apoptosis. To assess the effect of compound **18f**, loss of MMP was observed through fluorescence microscopy using rhodamine-123 staining. After 48 h treatment with compound **18f** against A549 cells, it was observed that the significant reduction in MMP at 3.0 μM was due to the decrease in fluorescence intensities that clearly justified the mitochondrial membrane destabilization in comparison to untreated cells. The result was quite similar in the case of the paclitaxel treatment group. The results obtained indicate the probable role of loss of MMP in the induction of apoptosis by **18f** in the A549 cell line (Figure 6).

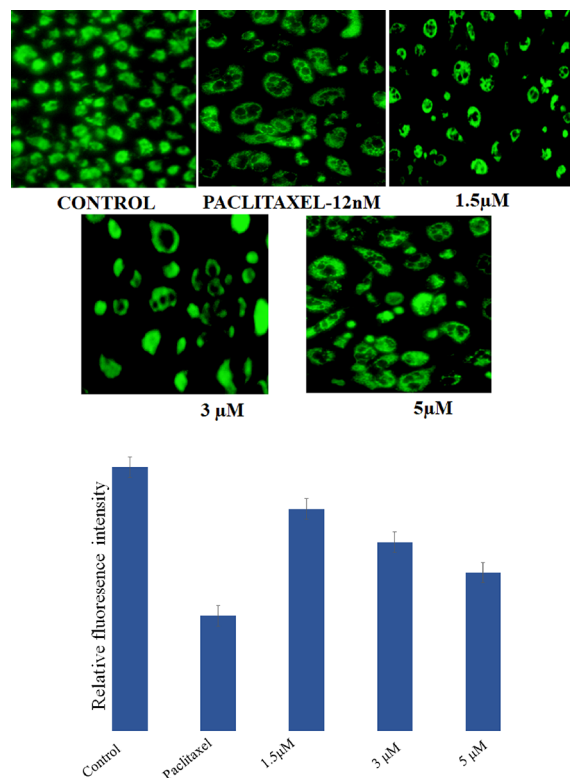


Figure 6. Effect of paclitaxel and **18f** on mitochondrial membrane potential using rhodamine-123. Exponentially growing A549 cells were treated with paclitaxel at its IC_{50} doses and **18f** at varying concentrations for 48 h. Paclitaxel was used as positive control. Cells treated with paclitaxel and **18f** at 5 μM show the maximum loss in the mitochondrial membrane potential.

Cell Cycle Analysis. To determine the effect of compound **18f** on the cell cycle of A549 cells, cell cycle analysis was performed using flow cytometry after 48 h of treatment. As shown in Figure 7, the treatment of compound **18f** induced the accumulation of cells in the S-phase from 31.78% in control to 50.57%, with a concomitant decrease in G0–G1 phase reduction from 62.8% in control to 34.32% in compound **18f** treated cells at 10 μM concentration (Figure 7).

Migration Potential of NCI-H460 and A549 Lung Cancer Cells. To determine the effect of compounds **14j** and **18f** on the migration capacities of NCI-H460 and A549 cells, a wound healing assay was performed. Compound **14j** showed moderate wound healing and inhibited the colony-forming ability of NCI-H460 cells (Figures S3 and S4). Our results demonstrated that doses of compound **18f** treatment at

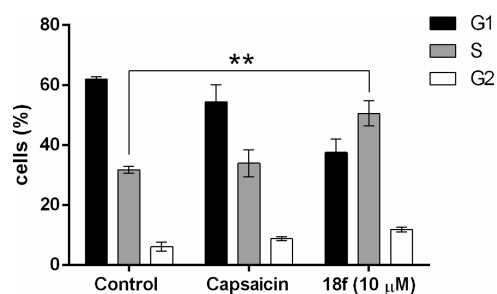


Figure 7. Compound **18f** induces cell cycle arrest in A549 cells. Cell cycle analysis of A549 cancer cells treated with compound **18f** for 48 h indicated that compound **18f** induced cell cycle arrest at the S-phase. Data presented as mean \pm SD of three independent experiments. $**P < 0.01$.

different concentrations significantly inhibited the migration potential of A549 cells when compared to their respective control group after 24 h of scratching (Figure 8).

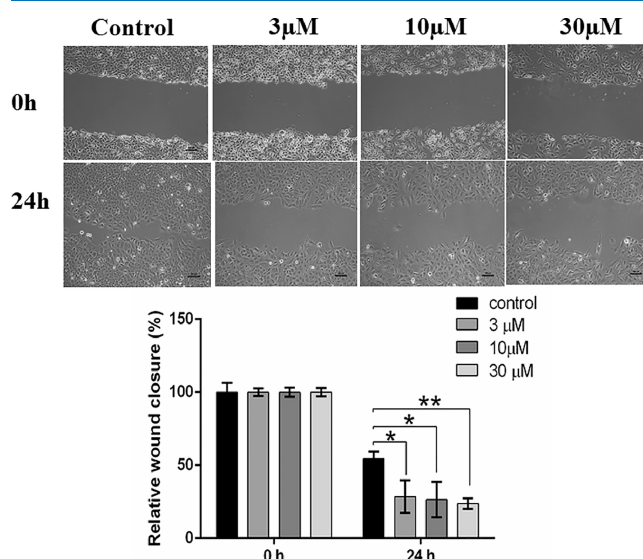


Figure 8. Compound **18f** inhibits the migration potential of A549 lung cancer cells. The migration potential of compound **18f** treated cells at different concentrations was examined using a wound healing assay. Images were captured at different time points, and the wound area was quantified using the ImageJ software. Scale bar, 100 μm ; magnification, 10 \times . $*P < 0.05$, $**P < 0.01$.

CONCLUSIONS

A series of thirty-one 1,2,3-triazole tethered capsaicinoids were synthesized by employing one-/two-point modifications around the capsaicin scaffold. All the newly synthesized compounds were evaluated for their antiproliferative activity against 60 cancer cell lines. Antiproliferative screening suggested that compounds **14g**, **14j**, **18b**, **18c**, **18f**, and **18m** showed good to moderate activity against cancer cell lines. The most potent compound (**18f**) showed good IC_{50} (2.92 μM) value against A549 non-small cell lung cancer. Compound **18f** revealed triggered apoptosis, elevated intracellular ROS levels, disrupted mitochondrial membrane potential and reduced cell migration potential of A549 cells in a dose-dependent manner. Further, compound **18f** was found to arrest the cell cycle at the S-phase and produced significant activity. As a result of the findings of this investigation, this compound may serve as a

template for the further development of novel capsacinoid-based anticancer agents against lung cancer.

METHODS

Chemistry. General Procedure for Synthesis of Propargylation. A solution of 0.5 g of compound (**10**) was dissolved in 10 mL of dry acetone followed by the addition of activated K_2CO_3 (5 equiv). Then propargyl bromide (1.2 equiv) was added to it and was refluxed for 4–5 h. After the completion of the reaction (monitored by TLC), the reaction mixture was allowed to attain room temperature and was poured into ice-cold water to form a colorless solid that was afterward filtered off under a vacuum to afford the desired product.

(E)-N-{3-Methoxy-4-(prop-2-yn-1-yloxy)benzyl}-8-methylnon-6-enamide (13**).** Pale yellow color solid, yield: 96%, 1H NMR (400 MHz, $DMSO-d_6$, ppm) δ 8.24 (s, 1H), 6.95 (d, J = 8.0 Hz, 1H), 6.87 (s, 1H), 6.75 (d, J = 8.4 Hz, 1H), 5.40–5.27 (m, 2H), 4.73 (d, J = 1.6 Hz, 2H), 4.19 (d, J = 5.6 Hz, 2H), 3.73 (s, 3H), 3.53 (s, 1H), 2.12 (t, J = 7.6 Hz, 2H), 1.94 (q, J = 6.8 Hz, 1H), 1.55–1.48 (m, 2H), 1.33–1.23 (m, 4H), 0.93 (d, J = 6.4 Hz, 4H), 0.84 (d, J = 6.8 Hz, 2H); MS (ESI) m/z : $[M + 1]^+$ 344.4; exact mass: 343.21; elemental analysis calculated for $(C_{21}H_{29}NO_3)$: C, 73.44; H, 8.51; N, 4.08; found: C, 73.39; H, 8.54; N, 4.10.

General Procedure for Synthesis of the 1,2,3-Triazole Ring (14a–p). The solution of compound (**13**) bearing terminal alkyne was dissolved in 15 mL of *t*-butanol/water (1:1) at ambient temperature. Then 1.5 equiv of $CuSO_4 \cdot 5H_2O$ was added, and the reaction mixture was stirred for 10 min. Initially, the color of the reaction mixture was observed to be light blue. Then sodium ascorbate (4 equiv) was added to the reaction mixture and allowed to stir for 15 min. The color of the reaction mixture changed from blue to dark brown. After 15 min, substituted aromatic azide (1.1 equiv) was added to the reaction mixture and was allowed to stir for a further 8 h at ambient temperature. After the completion of the reaction monitored by TLC, the reaction mixture was poured into the water and extracted with ethyl acetate (2×20 mL). The combined organic layer was dried over anhydrous sodium sulfate, filtered, and evaporated under reduced pressure to obtain the final triazole derivative (**14a–p**), which was recrystallized with ethyl acetate/hexane (70–90% quantitative yields).

(E)-N-(4-((1-(4-Chlorophenyl)-1H-1,2,3-triazol-4-yl)-methoxy)-3-methoxybenzyl)-8-methylnon-6-enamide (14a**).** Creamish solid, 94.0% yield; m.p. = 130.2 °C; 1H NMR (400 MHz, $CDCl_3$, ppm) δ 8.08 (s, 1H), 7.72–7.69 (d, J = 8.4 Hz, 2H), 7.53–7.51 (d, J = 8.4 Hz, 2H), 7.05–7.03 (d, J = 8.0 Hz, 1H), 6.87 (s, 1H), 6.83–6.81 (d, J = 8.4 Hz, 1H), 5.73 (s, 1H), 5.43–5.30 (m, 4H), 4.41–4.39 (d, J = 5.6 Hz, 2H), 3.89 (s, 3H), 2.25–2.21 (t, J = 6.8 Hz, 2H), 2.04–1.99 (q, J = 6.8 Hz, 1H), 1.72–1.65 (m, 2H), 1.45–1.38 (m, 4H), 0.98–0.97 (d, J = 6.8 Hz, 4H), 0.89–0.87 (d, J = 6.4 Hz, 2H); IR cm^{-1} : 3481, 3445, 3358, 3274, 3212, 3125, 3061, 3023, 2919, 2857, 1636, 1549, 1506, 1460, 1418, 1379, 1251, 1137, 1095, 1029, 971, 804, 762, 726, 656, 607; MS (ESI) m/z : $[M]^+$ 497.1; exact mass: 496.2241, elemental analysis calculated for $(C_{27}H_{33}ClN_4O_3)$: C, 65.25; H, 6.69; N, 11.27; found: C, 65.22; H, 6.70; N, 11.25.

(E)-N-(4-((1-(3-Chlorophenyl)-1H-1,2,3-triazol-4-yl)-methoxy)-3-methoxybenzyl)-8-methylnon-6-enamide (14b**).** Light brown solid, 87.0% yield; m.p. = 135.0 °C; 1H NMR

(400 MHz, $CDCl_3$, ppm) δ 8.10 (s, 1H), 7.81 (s, 1H), 7.66–7.64 (d, J = 7.6 Hz, 1H), 7.51–7.44 (m, 2H), 7.04–7.02 (d, J = 8.0 Hz, 1H), 6.87 (s, 1H), 6.83–6.81 (d, J = 8.0 Hz, 1H), 5.73 (s, 1H), 5.43–5.28 (m, 4H), 4.41–4.40 (d, J = 5.6 Hz, 2H), 3.89 (s, 3H), 2.26–2.23 (t, J = 7.6 Hz, 2H), 2.04–1.99 (q, J = 6.8 Hz, 1H), 1.70–1.66 (m, 2H), 1.43–1.28 (m, 4H), 0.98–0.96 (d, J = 6.8 Hz, 4H), 0.89–0.87 (d, J = 6.8 Hz, 2H); ^{13}C NMR (100 MHz, $CDCl_3$, ppm) δ 172.8 ($C=O$), 149.8 (triazolyl tertiary C), 146.8 (vanillyl Ar $C-OCH_3$), 145.3 (vanillyl Ar $C-OCH_2$), 138.1 ($-CH=CH-CH(CH_3)_2$), 137.8 (Ar C), 135.6 (Ar C), 132.4 (Ar C), 130.8 (vanillyl Ar $C-CH_2-NH$), 128.9 (Ar C), 126.4 ($-CH=CH-CH(CH_3)_2$), 121.0 (Ar C), 120.8 (vanillyl Ar C), 120.0 (triazolyl $-CH=C-N$), 118.5 (Ar C), 114.2 (vanillyl Ar C), 111.7 (vanillyl Ar C), 63.1 ($-OCH_2$), 55.9 ($-OCH_3$), 43.3 ($-CH_2NH$), 36.7 ($-COCH_2$), 32.2 ($-CH(CH_3)_2$), 30.9 ($-CH_2-CH=CH-CH(CH_3)_2$), 29.2 ($-CH_2-CH_2-CH=CH-CH(CH_3)_2$), 25.2 ($-COCH_2-CH_2$), 22.6 ($-CH(CH_3)_2$); IR cm^{-1} : 3421, 3288, 3180, 3121, 3091, 3006, 2955, 2924, 2893, 2852, 1629, 1593, 1506, 1456, 1322, 1217, 1137, 1027, 913, 846, 782, 666, 616, 531; MS (ESI) m/z : $[M]^+$ 497.1; exact mass: 496.2241, elemental analysis calculated for $(C_{27}H_{33}ClN_4O_3)$: C, 65.25; H, 6.69; N, 11.27; found: C, 65.22; H, 6.70; N, 11.25.

(E)-N-(4-((1-(2-Chlorophenyl)-1H-1,2,3-triazol-4-yl)-methoxy)-3-methoxybenzyl)-8-methylnon-6-enamide (14c**).** Creamish solid, 98.0% yield; m.p. = 88.6 °C; 1H NMR (400 MHz, $CDCl_3$, ppm) δ 8.09 (s, 1H), 7.63–7.58 (m, 2H), 7.50–7.44 (m, 2H), 7.05–7.03 (d, J = 12 Hz, 1H), 6.86 (s, 1H), 6.82–6.80 (d, J = 8.0 Hz, 2H), 5.86 (s, 1H), 5.42–5.29 (m, 4H), 4.39–4.38 (d, J = 5.6 Hz), 3.87 (s, 3H), 2.24–2.21 (t, J = 7.6 Hz, 2H), 2.01–1.98 (q, J = 6.8 Hz, 1H), 1.71–1.64 (m, 2H), 1.44–1.37 (m, 4H), 0.96 (d, J = 6.8 Hz, 4H), 0.87 (d, J = 6.8 Hz, 2H); ^{13}C NMR (100 MHz, $CDCl_3$, ppm): 172.9 ($C=O$), 149.9 (vanillyl Ar $C-OCH_3$), 146.9 (vanillyl Ar $C-OCH_2$), 144.0 (triazolyl tertiary C), 138.0 ($-CH=CH-CH(CH_3)_2$), 130.8 (Ar C), 130.7 (vanillyl Ar $C-CH_2-NH$), 128.6 (Ar C), 127.9 (Ar C), 127.7 (Ar C), 126.4 ($-CH=CH-CH(CH_3)_2$), 125.1 (Ar C), 120.0 (triazolyl $-CH=C-N$), 114.7 (vanillyl Ar C), 111.7 (Ar C), 63.2 ($-OCH_2$), 55.9 ($-OCH_3$), 43.3 ($-CH_2NH$), 36.6 ($-COCH_2$), 32.2 ($-CH(CH_3)_2$), 30.9 ($-CH_2-CH=CH-CH(CH_3)_2$), 29.2 ($-CH_2-CH_2-CH=CH-CH(CH_3)_2$), 25.2 ($-COCH_2-CH_2$), 22.6 ($-CH(CH_3)_2$); IR cm^{-1} : 3486, 3448, 3400, 3310, 3157, 3116, 3075, 3034, 2927, 2868, 2800, 1633, 1511, 1458, 1418, 1383, 1332, 1257, 1216, 1135, 1003, 851, 815, 756, 641, 606, 570, 544; MS (ESI) m/z : $[M]^+$ 497.1; exact mass: 496.2241, elemental analysis calculated for $(C_{27}H_{33}ClN_4O_3)$: C, 65.25; H, 6.69; N, 11.27; found: C, 65.22; H, 6.71; N, 11.025.

(E)-N-(4-((1-(3,4-Dichlorophenyl)-1H-1,2,3-triazol-4-yl)-methoxy)-3-methoxybenzyl)-8-methylnon-6-enamide (14d**).** Brown solid, 91.0% yield; m.p. = 131.1 °C; 1H NMR (400 MHz, $CDCl_3$, ppm) δ 8.09 (s, 1H), 7.91 (s, 1H), 7.62 (s, 1H), 7.01–6.99 (d, J = 4.4 Hz, 1H), 6.86 (s, 1H), 6.82–6.80 (d, J = 8.4 Hz, 1H), 5.83 (s, 1H), 5.42–5.29 (m, 4H), 4.40–4.38 (d, J = 5.6 Hz, 2H), 3.88 (s, 3H), 2.25–2.21 (t, J = 7.6 Hz, 2H), 2.03–1.98 (q, J = 6.4 Hz, 1H), 1.71–1.64 (m, 2H), 1.44–1.28 (m, 4H), 0.97–0.96 (d, J = 6.8 Hz, 4H), 0.88–0.86 (d, J = 6.8 Hz, 2H); ^{13}C NMR (100 MHz, $CDCl_3$, ppm) δ 172.9 ($C=O$), 149.7 (vanillyl Ar $C-OCH_3$), 146.7 (vanillyl Ar $C-OCH_2$), 145.5 (triazolyl tertiary C), 138.1 ($-CH=CH-CH(CH_3)_2$), 135.9 (Ar C), 134.0 (Ar C), 133.0 (Ar C), 132.4 (Ar C), 131.5 (vanillyl Ar $C-CH_2-NH$), 126.4 ($-CH=CH-CH(CH_3)_2$), 122.3 (Ar C), 120.9 (vanillyl Ar C), 120.0 (triazolyl $-CH=C-N$),

119.4(Ar **C**), 114.1(vanillyl Ar **C**), 111.6(vanillyl Ar **C**), 63.0(-OCH₂-), 55.9(-OCH₃-), 43.3(-CH₂NH-), 36.6(-COCH₂-), 32.2(-CH(CH₃)₂), 30.9(-CH₂-CH=CH-CH(CH₃)₂), 29.3(-CH₂-CH₂-CH=CH-CH(CH₃)₂), 25.2(-COCH₂-CH₂-), 22.6(-CH(CH₃)₂); IR cm⁻¹: 3436, 3343, 3306, 3276, 3209, 3113, 3075, 3017, 2928, 2888, 2819, 1742, 1699, 1638, 1515, 1456, 1420, 1393, 1318, 1232, 1136, 1026, 951, 811, 713, 664, 624, 591, 545; MS (ESI) *m/z*: [M + 2]⁺ 533.1; exact mass: 530.1851; elemental analysis calculated for (C₂₇H₃₂Cl₂N₄O₃): C, 61.02; H, 6.07; N, 10.54; found: C, 61.05; H, 6.05; N, 10.58.

(*E*)-*N*-(3-Methoxy-4-((1-(4-nitrophenyl)-1*H*-1,2,3-triazol-4-yl)methoxy)benzyl)-8-methylnon-6-enamide (**14e**). Creamish yellow solid, 95.0% yield; m.p. = 131.0 °C; ¹H NMR (400 MHz, CDCl₃, ppm) δ 8.45–8.23 (d, *J* = 8.8 Hz, 2H), 8.23 (s, 1H), 8.01–7.99 (d, *J* = 9.2 Hz, 2H), 7.04–7.02 (d, *J* = 8.0 Hz, 1H), 6.88 (s, 1H), 6.84–6.82 (d, *J* = 8.0 Hz, 1H), 5.75 (s, 1H), 5.43–5.30 (m, 4H), 4.41–4.40 (d, *J* = 5.6 Hz, 2H), 3.90 (s, 3H), 2.25–2.22 (t, *J* = 7.6 Hz, 2H), 2.04–1.99 (q, *J* = 6.8 Hz, 1H), 1.68–1.67 (m, 2H), 1.45–1.28 (m, 4H), 0.98–0.96 (d, *J* = 6.4 Hz, 4H), 0.89–0.87 (d, *J* = 6.4 Hz, 2H); ¹³C NMR (100 MHz, CDCl₃, ppm) δ 173.0(C=O), 149.7(vanillyl Ar **C**-OCH₃), 148.7(Ar **C**-NO₂), 147.2(vanillyl Ar **C**-OCH₂-), 146.6 (triazolyl tertiary **C**), 141.5(Ar **C**), 138.1(-CH=CH-CH(CH₃)₂), 132.6(vanillyl Ar **C**-CH₂-NH-), 126.4(-CH=CH-CH(CH₃)₂), 125.5(Ar **C**), 120.5(triazolyl -CH=C-N-), 119.9(Ar **C**), 114.1(vanillyl Ar **C**), 111.6(vanillyl Ar **C**), 63.0(-OCH₂-), 55.9(-OCH₃-), 43.2(-CH₂NH-), 36.6(-COCH₂-), 32.2(-CH(CH₃)₂), 30.9(-CH₂-CH=CH-CH(CH₃)₂), 29.2(-CH₂-CH₂-CH=CH-CH(CH₃)₂), 25.2(-COCH₂-CH₂-), 22.6(-CH(CH₃)₂); IR cm⁻¹: 3415, 3316, 3246, 3201, 3102, 3049, 2988, 2923, 2860, 2829, 1672, 1635, 1599, 1551, 1515, 1463, 1341, 1258, 1229, 1136, 1021, 851, 816, 748, 684, 644, 600, 542; MS (ESI) *m/z*: [M + 1]⁺ 508.1; exact mass: 507.2481; elemental analysis calculated for (C₂₇H₃₃N₅O₅): C, 63.89; H, 6.55; N, 13.80; found: C, 63.85; H, 6.58; N, 13.84.

(*E*)-*N*-(3-Methoxy-4-((1-(3-nitrophenyl)-1*H*-1,2,3-triazol-4-yl)methoxy)benzyl)-8-methylnon-6-enamide (**14f**). Creamish brown, 93.0% yield; m.p. = 164.7 °C; ¹H NMR (400 MHz, CDCl₃, ppm) δ 8.63 (s, 1H), 8.33–8.32 (d, *J* = 7.2 Hz, 1H), 8.23–8.39 (m, 2H), 7.80–7.76 (m, 1H), 7.02–6.99 (d, *J* = 11.2 Hz, 1H), 6.88 (s, 1H), 6.83–6.82 (d, *J* = 6.4 Hz, 1H), 5.76 (s, 1H), 5.39 (s, 4H), 4.40–4.42 (d, *J* = 6.4 Hz, 2H), 3.90 (s, 3H), 2.24 (s, 2H), 2.02–2.00 (m, 1H), 1.69 (s, 2H), 1.43–1.28 (m, 4H), 0.98–0.97 (d, *J* = 5.6 Hz, 4H), 0.89–0.88 (d, *J* = 5.2 Hz, 2H); IR cm⁻¹: 3499, 3451, 3377, 3327, 3261, 3193, 3152, 3110, 3057, 2941, 2856, 2830, 1635, 1531, 1458, 1346, 1258, 1224, 1137, 1083, 1029, 971, 797, 732, 662, 589, 545; MS (ESI) *m/z*: [M + 1]⁺ 508.2; exact mass: 507.2481; elemental analysis calculated for (C₂₇H₃₃N₅O₅): C, 63.89; H, 6.55; N, 13.80; found: C, 63.92; H, 6.55; N, 13.78.

(*E*)-*N*-(3-Methoxy-4-((1-(4-(trifluoromethyl)phenyl)-1*H*-1,2,3-triazol-4-yl)methoxy)benzyl)-8-methylnon-6-enamide (**14g**). Creamish brown, 89.0% yield; m.p. = 156.3 °C; ¹H NMR (400 MHz, CDCl₃, ppm) δ 8.17 (s, 1H), 8.05 (s, 1H), 7.97–7.96 (d, *J* = 8.0 Hz, 1H), 7.75–7.68 (m, 2H), 7.04–7.02 (d, *J* = 8.0 Hz, 1H), 6.87 (s, 1H), 6.83–6.81 (d, *J* = 8.0 Hz, 1H), 5.79 (s, 1H), 5.42–5.30 (m, 4H), 4.404.39 (d, *J* = 6.0 Hz, 2H), 3.89 (s, 3H), 7.27–2.23 (t, *J* = 7.6 Hz, 2H), 2.03–1.98 (q, *J* = 6.8 Hz, 1H), 1.72–1.64 (m, 2H), 1.45–1.28 (m, 4H), 0.98–0.96 (d, *J* = 6.8 Hz, 4H), 0.88–0.87 (d, *J* = 6.4 Hz, 2H); ¹³C NMR (100 MHz, CDCl₃, ppm) δ 172.9(C=O),

149.7(vanillyl Ar **C**-OCH₃), 146.7(vanillyl Ar **C**-OCH₂-), 145.5(triazolyl tertiary **C**), 138.0(-CH=CH-CH(CH₃)₂), 137.2(Ar **C**), 132.5(Ar **C**), 130.5(vanillyl Ar **C**-CH₂-NH-), 126.4(-CH=CH-CH(CH₃)₂), 125.4(vanillyl Ar **C**), 123.5(Ar **C**), 121.4(Ar **C**), 119.9(triazolyl -CH=C-N-), 117.4(Ar **C**), 114.2(vanillyl Ar **C**), 111.6(vanillyl Ar **C**), 63.0 (-OCH₂-), 55.8 (OCH₃), 43.2(CH₂NH-), 36.6(-COCH₂-), 32.2(-CH(CH₃)₂), 30.9(-CH₂-CH=CH-CH(CH₃)₂), 29.2(-CH₂-CH₂-CH=CH-CH(CH₃)₂), 25.2(-COCH₂-CH₂-), 22.6(-CH(CH₃)₂); IR cm⁻¹: 3492, 3415, 3373, 3274, 3209, 3178, 3151, 3128, 3089, 3046, 2926, 2856, 2809, 1638, 1546, 1512, 1459, 1326, 1260, 1229, 1167, 1119, 1029, 966, 891, 832, 795, 736, 690, 593, 547; MS (ESI) *m/z*: [M + 1]⁺ 531.1; exact mass: 530.2504; elemental analysis calculated for (C₂₈H₃₃F₃N₄O₃): C, 63.38; H, 6.27; N, 10.56; found: C, 63.35; H, 6.25; N, 10.55.

(*E*)-*N*-(4-((1-(4-Fluorophenyl)-1*H*-1,2,3-triazol-4-yl)-methoxy)-3-methoxybenzyl)-8-methylnon-6-enamide (**14h**). Brown solid, 95.0% yield; m.p. = 118.0 °C; ¹H NMR (400 MHz, CDCl₃, ppm) δ 8.11 (s, 1H), 7.79–7.75 (m, 2H), 7.31–7.27 (t, *J* = 8.4 Hz, 2H), 7.10–7.04 (d, *J* = 8.0 Hz, 1H), 6.92 (s, 1H), 6.88–6.86 (d, *J* = 8.0 Hz, 1H), 5.83 (s, 1H), 5.47–5.35 (m, 4H), 4.45–4.44 (d, *J* = 5.6 Hz, 2H), 3.93 (s, 3H), 2.30–2.26 (t, *J* = 7.2 Hz, 2H), 2.08–2.03 (q, *J* = 6.8 Hz, 1H), 1.77–1.69 (m, 2H), 1.50–1.33 (m, 4H), 1.03–1.01 (d, *J* = 6.8 Hz, 4H), 0.93–0.92 (d, *J* = 6.4 Hz, 2H); ¹³C NMR (100 MHz, CDCl₃, ppm) δ 172.9(C=O), 163.7(Ar **C**-F), 149.7(vanillyl Ar **C**-OCH₃), 146.8(vanillyl Ar **C**-OCH₂-), 145.1(triazolyl tertiary **C**), 138.0(-CH=CH-CH(CH₃)₂), 133.2(Ar **C**), 132.3(vanillyl Ar **C**-CH₂-NH-), 126.4(-CH=CH-CH(CH₃)₂), 122.6(Ar **C**), 122.5(Ar **C**), 120.0(triazolyl -CH=C-N-), 116.8(Ar **C**), 116.6(Ar **C**), 114.1(vanillyl Ar **C**), 111.6(vanillyl Ar **C**), 63.1(OCH₂), 55.9(OCH₃), 43.3(CH₂NH), 38.9(COCH₂), 36.6(-COCH₂-), 32.2(-CH(CH₃)₂), 30.9(-CH₂-CH=CH-CH(CH₃)₂), 29.6(-CH₂-CH₂-CH=CH-CH(CH₃)₂), 25.2(-COCH₂-CH₂-), 22.6(-CH(CH₃)₂); IR cm⁻¹: 3472, 3418, 3393, 3326, 3282, 3181, 3147, 3076, 3036, 2922, 2864, 1635, 1512, 1458, 1416, 1259, 1224, 1136, 1017, 834, 801, 752, 709, 605, 543; MS (ESI) *m/z*: [M + 1]⁺ 481.1; exact mass: 480.2536; elemental analysis calculated for (C₂₇H₃₃FN₄O₃): C, 67.48; H, 6.92; N, 11.66; found: C, 67.45; H, 6.90; N, 11.69.

(*E*)-*N*-(4-((1-(2-Fluorophenyl)-1*H*-1,2,3-triazol-4-yl)-methoxy)-3-methoxybenzyl)-8-methylnon-6-enamide (**14i**). Creamish solid, 93.0% yield; m.p. = 113.0 °C; ¹H NMR (400 MHz, CDCl₃, ppm) δ 8.21 (d, *J* = 2.4 Hz, 1H), 8.0–7.96 (dd, *J* = 7.6 and 1.6 Hz, 1H), 7.47–7.45 (m, 1H), 7.37–7.32 (m, 1H), 7.08–7.06 (d, *J* = 8.0 Hz, 1H), 6.87 (s, 1H), 6.84–6.82 (d, *J* = 8.0 Hz, 1H), 5.68 (s, 1H), 5.43–5.30 (m, 4H), 4.41–4.40 (d, *J* = 6.0 Hz, 2H), 3.89 (s, 1H), 2.27–2.21 (t, *J* = 7.2 Hz, 2H), 2.04–1.99 (q, *J* = 6.8 Hz, 1H), 1.73–1.65 (m, 2H), 1.46–1.28 (m, 4H), 0.98–0.97 (d, *J* = 6.8 Hz, 4H), 0.89–0.07 (d, *J* = 6.8 Hz, 2H); ¹³C NMR (100 MHz, CDCl₃, ppm) δ 172.9(C=O), 149.7(vanillyl Ar **C**-OCH₃), 147.3(vanillyl Ar **C**-OCH₂-), 146.7(triazolyl tertiary **C**), 141.0(vanillyl Ar **C**), 138.1(-CH=CH-CH(CH₃)₂), 132.6(vanillyl Ar **C**-CH₂-NH-), 126.4(-CH=CH-CH(CH₃)₂), 125.5(Ar **C**), 120.9(Ar **C**), 120.5(triazolyl -CH=C-N-), 119.9(Ar **C**), 114.2(vanillyl Ar **C**), 111.6(vanillyl Ar **C**), 63.0(-OCH₂-), 55.9(-OCH₃-), 43.2(-CH₂NH-), 36.8(-COCH₂-), 32.2(-CH(CH₃)₂), 30.9(-CH₂-CH=CH-CH(CH₃)₂), 29.6(-CH₂-CH₂-CH=CH-CH(CH₃)₂), 25.2(-COCH₂-CH₂-), 22.6(-CH(CH₃)₂); IR cm⁻¹: 3476, 3414, 3367, 3293, 3245, 3212, 3083, 3046, 3016, 2918, 2860, 1672, 1633, 1515, 1462, 1419, 1359, 1261, 1234, 1135,

1038, 995, 853, 802, 751, 641; MS (ESI) m/z : $[M + 1]^+$ 481.1; exact mass: 480.2536; elemental analysis calculated for $(C_{27}H_{33}FN_4O_3)$: C, 67.48; H, 6.92; N, 11.66; found: C, 67.45; H, 6.95; N, 11.61.

(*E*)-*N*-(4-((1-(4-Cyanophenyl)-1*H*-1,2,3-triazol-4-yl)methoxy)-3-methoxybenzyl)-8-methylnon-6-enamide (**14j**). Light gray solid, 84.0% yield; m.p. = 178.3 °C; 1H NMR (400 MHz, $CDCl_3$, ppm) δ 8.18 (s, 1H), 8.00 (s, 2H), 7.86 (s, 1H), 7.10 (s, 1H), 7.04 (s, 1H), 6.88 (s, 1H), 6.83 (s, 1H), 5.75 (s, 1H), 5.39–5.34 (m, 4H), 4.40 (s, 2H), 3.89 (s, 3H), 2.23 (s, 2H), 2.01 (s, 1H), 1.68 (s, 2H), 1.46–1.28 (m, 4H), 0.98–0.97 (d, J = 6.4 Hz, 4H), 0.89–0.87 (d, J = 6.8 Hz, 2H); IR cm^{-1} : 3470, 3390, 3343, 3302, 3257, 3150, 3079, 3029, 2956, 2923, 2857, 1628, 1513, 1454, 1414, 1365, 1257, 1220, 1134, 1018, 842, 793, 667, 619, 535; MS (ESI) m/z : $[M + 1]^+$ 488.1; exact mass: 487.2583; elemental analysis calculated for $(C_{28}H_{33}N_5O_3)$: C, 68.97; H, 6.82; N, 14.36; found: C, 68.98; H, 6.86; N, 14.35.

(*E*)-*N*-(4-((1-(4-Bromophenyl)-1*H*-1,2,3-triazol-4-yl)methoxy)-3-methoxybenzyl)-8-methylnon-6-enamide (**14k**). Brown solid, 91.0% yield; m.p. = 127.8 °C; 1H NMR (400 MHz, $CDCl_3$, ppm) δ 8.09 (s, 1H), 7.68–7.62 (q, J = 7.2 Hz, 4H), 7.03–7.01 (d, J = 8.0 Hz, 1H), 6.86 (s, 1H), 6.81–6.79 (d, J = 8.0 Hz, 1H), 5.86 (s, 1H), 5.42–5.29 (m, 4H), 4.39–4.38 (d, J = 5.6 Hz, 2H), 3.87 (s, 3H), 2.24–2.21 (t, J = 7.2 Hz, 2H), 2.03–1.98 (q, J = 6.4 Hz, 1H), 1.71–1.63 (m, 2H), 1.44–1.28 (m, 4H), 0.97–0.96 (d, J = 6.8 Hz, 4H), 0.88–0.86 (d, J = 6.8 Hz, 2H); ^{13}C NMR (100 MHz, $CDCl_3$, ppm) δ 173.0($\underline{C=O}$), 149.7(vanillyl Ar $\underline{C-OCH_3}$), 146.7(vanillyl Ar $\underline{C-OCH_2-}$), 138.0(triazolyl tertiary \underline{C}), 135.8($\underline{CH=CH-CH(CH_3)_2}$), 132.9(Ar \underline{C}), 132.4(vanillyl Ar $\underline{C-CH_2-NH-}$), 126.4($\underline{CH=CH-CH(CH_3)_2}$), 122.5(Ar \underline{C}), 121.9(Ar \underline{C}), 121.1(triazolyl $\underline{CH=C-N-}$), 119.9(Ar \underline{C}), 114.1(vanillyl Ar \underline{C}), 111.6(vanillyl Ar \underline{C}), 63.0($\underline{OCH_2-}$), 55.8($\underline{OCH_3}$), 43.2($\underline{CH_2NH-}$), 36.6($\underline{COCH_2-}$), 32.2($\underline{CH(CH_3)_2}$), 30.9($\underline{CH_2-CH=CH-CH(CH_3)_2}$), 29.2($\underline{CH_2-CH_2-CH=CH-CH(CH_3)_2}$), 25.2($\underline{COCH_2-CH_2-}$), 22.6($\underline{CH(CH_3)_2}$); IR cm^{-1} : 3461, 3410, 3371, 3291, 3227, 3159, 3056, 3025, 2957, 2924, 2863, 1638, 1593, 1508, 1459, 1415, 1325, 1258, 1231, 1137, 1012, 799, 727, 692, 613, 567, 519; MS (ESI) m/z : $[M]^+$ 541, $[M + 1]^+$ 542, $[M + 2]^+$ 543; exact mass: 540.1736; elemental analysis calculated for $(C_{27}H_{33}BrN_4O_3)$: C, 59.86; H, 6.14; N, 10.35; found: C, 59.85; H, 6.17; N, 10.38.

(*E*)-*N*-(3-Methoxy-4-((1-(2-methoxyphenyl)-1*H*-1,2,3-triazol-4-yl)methoxy)benzyl)-8-methylnon-6-enamide (**14l**). Light gray, 97.0% yield; m.p. = 112.6 °C; 1H NMR (400 MHz, $CDCl_3$, ppm) δ 8.23 (s, 1H), 7.80–7.78 (dd, J = 7.6 and 1.6 Hz, 1H), 7.47–7.42 (m, 1H), 7.14–7.07 (m, 3H), 6.86 (s, 1H), 6.83–6.81 (d, J = 8.0 Hz, 1H), 5.78 (s, 1H), 5.42–5.30 (m, 4H), 4.40–4.39 (d, J = 5.6 Hz, 2H), 3.90 (s, 3H), 3.88 (s, 3H), 2.26–2.23 (t, J = 7.2 Hz), 2.03–1.98 (q, J = 6.8 Hz, 1H), 1.72–1.64 (m, 2H), 1.45–1.28 (m, 4H), 0.98–0.696 (d, J = 6.8 Hz, 4H), 0.89–0.87 (d, J = 6.4 Hz, 2H); ^{13}C NMR (100 MHz, $CDCl_3$, ppm) δ 172.9($\underline{C=O}$), 151.1(Ar $\underline{C-OCH_3}$), 149.8(vanillyl Ar $\underline{C-OCH_3}$), 147.0(vanillyl Ar $\underline{C-OCH_2-}$), 143.4(triazolyl tertiary \underline{C}), 138.0($\underline{CH=CH-CH(CH_3)_2}$), 132.1(Ar \underline{C}), 130.1(vanillyl Ar $\underline{C-CH_2-NH-}$), 126.4(Ar \underline{C}), 126.2($\underline{CH=CH-CH(CH_3)_2}$), 125.4(Ar \underline{C}), 125.3(Ar \underline{C}), 121.2(Ar \underline{C}), 120.0(triazolyl $\underline{CH=C-N-}$), 114.4(vanillyl Ar \underline{C}), 112.2(vanillyl Ar \underline{C}), 111.6(vanillyl Ar \underline{C}), 63.2($\underline{OCH_2}$), 55.9($\underline{OCH_3}$), 43.3($\underline{CH_2NH}$), 36.7($\underline{COCH_2-}$), 32.2($\underline{CH(CH_3)_2}$), 30.9($\underline{CH_2-CH=CH-CH(CH_3)_2}$), 29.3($\underline{CH_2-CH_2-CH=CH-CH(CH_3)_2}$), 25.2($\underline{COCH_2-CH_2-}$), 22.6($\underline{CH-$

$\underline{CH_3)_2}$); IR cm^{-1} : 3476, 3449, 3404, 3314, 3269, 3173, 3108, 3045, 3017, 2996, 2928, 2874, 2836, 1634, 1601, 1538, 1509, 1464, 1418, 1388, 1254, 1215, 1137, 1046, 1010, 852, 823, 754, 691, 639, 583, 549; MS (ESI) m/z : $[M + 1]^+$ 493.1; exact mass: 492.2736; elemental analysis calculated for $(C_{28}H_{36}N_4O_4)$: C, 68.27; H, 7.37; N, 11.37; found: C, 68.30; H, 7.34; N, 11.40.

(*E*)-*N*-(3-Methoxy-4-((1-(3,4,5-trimethoxyphenyl)-1*H*-1,2,3-triazol-4-yl)methoxy)benzyl)-8-methylnon-6-enamide (**14m**). Brown solid, 89.0% yield; m.p. = 106.2 °C; 1H NMR (400 MHz, $CDCl_3$, ppm) δ 8.07 (s, 1H), 7.06–7.04 (d, J = 8.4 Hz, 1H), 6.96 (s, 2H), 6.87 (s, 1H), 6.83–6.81 (d, J = 8.0 Hz, 1H), 5.77 (s, 1H), 5.42–5.30 (m, 4H), 4.41–4.39 (d, J = 5.6 Hz, 2H), 3.95 (s, 9H), 3.91 (s, 3H), 3.95–3.89 (d, J = 8.4 Hz, 1H), 1.68–1.66 (d, J = 6.8 Hz, 2H), 1.43–1.39 (t, J = 8.0 Hz, 4H), 0.98–0.96 (d, J = 6.8 Hz, 4H), 0.88–0.87 (d, J = 6.8 Hz, 2H); ^{13}C NMR (100 MHz, $CDCl_3$, ppm) δ 172.9($\underline{C=O}$), 153.9(triazolyl tertiary \underline{C}), 149.7(vanillyl Ar $\underline{C-OCH_3}$), 146.9(vanillyl Ar $\underline{C-OCH_2-}$), 138.4(Ar \underline{C}), 138.1($\underline{CH=CH-CH(CH_3)_2}$), 132.8(Ar \underline{C}), 132.3(vanillyl Ar $\underline{C-CH_2-NH-}$), 126.4($\underline{CH=CH-CH(CH_3)_2}$), 121.4(Ar \underline{C}), 120.0(triazolyl $\underline{CH=C-N-}$), 114.1(vanillyl Ar \underline{C}), 111.6(vanillyl Ar \underline{C}), 63.2($\underline{OCH_3}$), 61.0($\underline{OCH_2}$), 56.4($\underline{OCH_3}$), 55.9($\underline{OCH_3}$), 43.3($\underline{CH_2NH}$), 36.6($\underline{COCH_2-}$), 32.2($\underline{CH(CH_3)_2}$), 30.9($\underline{CH_2-CH=CH-CH(CH_3)_2}$), 29.3($\underline{CH_2-CH_2-CH=CH-CH(CH_3)_2}$), 25.2($\underline{COCH_2-CH_2-}$), 22.6($\underline{CH(CH_3)_2}$); IR cm^{-1} : 3492, 3461, 3407, 3319, 3253, 3192, 3135, 3072, 3020, 2954, 2922, 2890, 2848, 1635, 1598, 1510, 1460, 1414, 1226, 1124, 1032, 1000, 861, 810, 737, 689, 644, 613, 558; MS (ESI) m/z : $[M + 1]^+$ 553.1; exact mass: 552.2947; elemental analysis calculated for $(C_{30}H_{40}N_4O_4)$: C, 65.20; H, 7.30; N, 10.14; found: C, 65.22; H, 7.35; N, 10.12.

(*E*)-*N*-(3-Methoxy-4-((1-(*p*-tolyl)-1*H*-1,2,3-triazol-4-yl)methoxy)benzyl)-8-methylnon-6-enamide (**14n**). Creamish solid, 94.0% yield; m.p. = 115.4 °C; 1H NMR (400 MHz, $CDCl_3$, ppm) δ 8.06 (s, 1H), 7.63–7.61 (d, J = 8.4 Hz, 2H), 7.35–7.33 (d, J = 8 Hz, 2H), 7.07–7.05 (d, J = 8.4 Hz, 1H), 6.87 (s, 1H), 6.83–6.81 (d, J = 8 Hz, 1H), 5.70 (s, 1H), 5.43–5.30 (m, 4H), 4.41–4.39 (d, J = 5.6 Hz, 2H), 3.89 (s, 3H), 2.45 (s, 3H), 2.25–2.21 (t, J = 7.2 Hz, 2H), 2.02–2.01 (q, J = 6.8 Hz, 1H), 1.68–1.65 (m, 2H), 1.45–1.38 (m, 4H), 0.98–0.97 (d, J = 6.8 Hz, 4H), 0.89–0.87 (d, J = 6.4 Hz, 2H); IR cm^{-1} : 3461, 3411, 3377, 3306, 3233, 3173, 3146, 3123, 3025, 2957, 2926, 2870, 2809, 1632, 1516, 1460, 1414, 1258, 1218, 1161, 1134, 1096, 1037, 992, 847, 805, 709, 679, 637, 603, 573, 526; MS (ESI) m/z : $[M + 1]^+$ 477.2; exact mass: 476.2787; elemental analysis calculated for $(C_{28}H_{36}N_4O_4)$: C, 70.56; H, 7.61; N, 11.76; found: C, 70.55; H, 7.64; N, 11.8.

(*E*)-*N*-(4-((1-(4-Ethylphenyl)-1*H*-1,2,3-triazol-4-yl)methoxy)-3-methoxybenzyl)-8-methylnon-6-enamide (**14o**). Creamish brown solid, 90.0% yield; m.p. = 105.1 °C; 1H NMR (400 MHz, $CDCl_3$, ppm) δ 8.06 (s, 1H), 7.65–7.63 (d, J = 8.4 Hz, 2H), 7.37–7.35 (d, J = 8.4 Hz, 2H), 7.06–7.04 (d, J = 8.0 Hz, 1H), 6.86 (s, 1H), 6.83–6.80 (d, J = 8 Hz, 1H), 5.76 (s, 1H), 5.42–5.30 (m, 4H), 4.40–4.39 (d, J = 5.6 Hz, 2H), 3.88 (s, 3H), 2.77–2.71 (q, J = 7.6 Hz, 2H), 2.25–2.21 (t, J = 7.6 Hz, 3H), 2.03–1.98 (q, J = 6.4 Hz, 2H), 1.72–1.64 (m, 2H), 1.45–1.37 (m, 1H), 1.32–1.28 (t, J = 7.6 Hz, 4H), 0.98–0.96 (d, J = 6.8 Hz, 4H), 0.89–0.87 (d, J = 6.4 Hz, 2H); ^{13}C NMR (100 MHz, $CDCl_3$, ppm) δ 172.8($\underline{C=O}$), 149.7(vanillyl Ar $\underline{C-OCH_3}$), 146.9(vanillyl Ar $\underline{C-OCH_2-}$), 145.3(triazolyl tertiary \underline{C}), 144.7(vanillyl Ar \underline{C}), 138.0($\underline{CH=CH-CH(CH_3)_2}$),

134.8(Ar C), 132.2(vanillyl Ar C-CH₂-NH-), 129.1(Ar C), 126.4(-CH=CH-CH(CH₃)₂), 121.2(Ar C), 120.6(Ar C), 120.0(triazolyl -CH=C-N-), 114.2(vanillyl Ar C), 111.6(vanillyl Ar C), 63.1(-OCH₂-), 55.9(-OCH₃), 43.3(-CH₂NH-), 36.8(-COCH₂-), 36.7(Ar CH₂CH₃), 32.2(-CH(CH₃)₂), 30.9(-CH₂-CH=CH-CH(CH₃)₂), 29.3(-CH₂-CH₂-CH=CH-CH(CH₃)₂), 25.2(-COCH₂-CH₂-), 22.6(-CH(CH₃)₂), 15.4(Ar CH₂CH₃); IR cm⁻¹: 3486, 3428, 3381, 3300, 3277, 3239, 3190, 3148, 3043, 2959, 2921, 2865, 1634, 1515, 1457, 1418, 1326, 1255, 1136, 1035, 993, 804, 733, 670, 603, 578, 541; MS (ESI) *m/z*: [M + 1]⁺ 491.1, exact mass: 490.2943; elemental analysis calculated for (C₂₈H₃₆N₄O₄): C, 70.99; H, 7.81; N, 11.42; found: C, 70.95; H, 7.82; N, 11.45.

(*E*)-*N*-(4-((1-(3,4-Dimethylphenyl)-1*H*-1,2,3-triazol-4-yl)-methoxy)-3-methoxybenzyl)-8-methylnon-6-enamide (**14p**). Creamish solid, 97.0% yield; m.p. = 109.1 °C; ¹H NMR (400 MHz, CDCl₃, ppm) δ 8.05 (s, 1H), 7.53 (s, 1H), 7.43–7.41 (d, *J* = 8.0 Hz, 1H), 7.29–7.28 (d, *J* = 2.4 Hz, 1H), 7.06–7.04 (d, *J* = 8.4 Hz, 1H), 6.87 (s, 1H), 6.83–6.81 (d, *J* = 8.0 Hz, 1H), 5.73 (s, 1H), 5.43–5.30 (m, 4H), 4.40–4.39 (d, *J* = 5.6 Hz, 2H), 3.89 (s, 3H), 2.37–2.34 (d, *J* = 8.4 Hz, 6H), 2.26–2.21 (t, *J* = 7.6 Hz, 2H), 2.04–1.99 (q, *J* = 6.8 Hz, 1H), 1.72–1.64 (m, 2H), 1.45–1.28 (m, 4H), 0.98–0.06 (d, *J* = 6.8 Hz, 4H), 0.89–0.87 (d, *J* = 6.8 Hz, 2H); IR cm⁻¹: 3494, 3461, 3425, 3384, 3360, 3300, 3248, 3140, 3056, 3028, 2927, 2876, 1633, 1512, 1461, 1414, 1336, 1258, 1217, 1136, 1041, 990, 878, 848, 807, 699, 634, 596; MS (ESI) *m/z*: [M + 1]⁺ 493.1; exact mass: 490.2943; elemental analysis calculated for (C₂₈H₃₆N₄O₄): C, 70.99; H, 7.81; N, 11.42; found: C, 70.98; H, 7.85; N, 11.45.

4-Hydroxy-3-methoxybenzaldehyde Oxime (16a). A solution of 1 g of hydroxylamine hydrochloride and sodium acetate trihydrate (2 equiv) was dissolved in 25 mL of water. Further on, vanillin (15, 0.9 equiv) was added to the reaction mixture and refluxed for 10 min. After the completion of the reaction monitored by TLC, the reaction mixture was brought to room temperature. The solid precipitate formed was filtered off under a vacuum and washed with 10 mL of cold water that led to the colorless solid in pure form in 76.4% quantitative yield. Melting point (m.p.) = 79.3 °C; ¹H NMR (400 MHz, CDCl₃, ppm) δ 9.10 (s, 1H), 8.03 (s, 1H), 7.69 (s, 1H), 7.10–7.04 (m, 1H), 6.87 (d, *J* = 8.4 Hz, 1H), 3.86 (s, 3H); exact mass: 167.06, elemental analysis calculated for (C₈H₉NO₃): C, 57.48; H, 5.43; N, 8.38; found: C, 57.47; H, 5.45; N, 8.37.

4-Hydroxy-3-methoxy-phenylamine (16b). A solution of 1 g of 4-hydroxy-3-methoxy-benzaldehyde oxime (**16a**) in 5 mL of acetic acid was cooled to 10–15 °C. Then 4.71 g (4 equiv) of activated zinc dust was added to the reaction mixture and stirred at ambient temperature for a further 3 h. Completion of the reaction was monitored by TLC, and the reaction mixture was filtered off to remove excess zinc. Further on, the filtrate was collected and neutralized with ammonia to yield a white solid precipitate. The precipitate formed was filtered under a vacuum and washed with 20 mL of cold water to afford the required compound (**16b**) in pure form (74.0% yield) that was directly used for the next step without any further purification. ¹H NMR (400 MHz, CDCl₃, ppm) δ 6.83 (ddt, *J* = 8.8, 1.7, 0.9 Hz, 1H), 6.82–6.76 (m, 2H), 6.61 (s, 1H), 3.93 (tt, *J* = 6.2, 0.9 Hz, 2H), 3.85 (s, 2H), 1.39 (d, *J* = 12.5 Hz, 1H). Chemical formula: C₈H₁₁NO₂, elemental analysis: C, 62.73; H, 7.24; N, 9.14. found: C, 62.76; H, 7.29; N, 9.19.

General Procedure for *N*-(4-Hydroxy-3-methoxybenzyl)-3,7-dimethyloct-6-enamide (16c). To the DMF (10 mL)

solution of *R*-(+)-citronellic acid (1.2 equiv), 2 equiv of (3-dimethylamino-propyl)-ethyl-carbodiimide hydrochloride (EDC·HCl) and 0.2 equiv of hydroxybenzotriazole (HOBT) were added, and the reaction mixture was stirred for 5 min under an inert atmosphere in a two-neck round-bottom flask. Finally, the compound (**16b**) was added in the reaction mixture to continue at room temperature overnight. The completion of the reaction was monitored by TLC; the reaction mixture was poured into ice-cold water and extracted with ethyl acetate (4 × 20 mL). The combined organic layers were dried over anhydrous sodium sulfate, filtered, and evaporated under a vacuum to afford the impure reaction mixture that was purified by column chromatography (silica gel) to obtain the pure natural product hybrid amide. ¹H NMR (400 MHz, CDCl₃, ppm) δ 6.86–6.81 (m, 2H), 6.78 (m, 1H), 6.57 (s, 1H), 5.12–5.04 (m, 1H), 4.38 (m, 2H), 3.85 (s, 2H), 2.49 (d, *J* = 16.2 Hz, 1H), 2.25 (d, *J* = 16.2 Hz, 1H), 2.10–2.00 (m, 1H), 2.03–1.80 (m, 2H), 1.66 (m, 3H), 1.53 (m, 1H), 1.27 (m, 1H), 0.97 (d, *J* = 8.1 Hz, 3H); exact mass: 305.20; elemental analysis calculated for (C₁₈H₂₇NO₃): C, 70.79; H, 8.91; N, 4.59; O, 15.72; found: C, 70.77; H, 9.93; N, 4.57.

***N*-(3-Methoxy-4-(prop-2-yn-1-yloxy)benzyl)-3,7-dimethyloct-6-enamide (17).** A solution of 0.5 g compound (**16c**) was dissolved in 10 mL of dry acetone followed by the addition of activated K₂CO₃ (5 equiv). Then propargyl bromide (1.2 equiv) was added to it and refluxed for 4–5 h. After the completion of the reaction (monitored by TLC), the reaction mixture was allowed to attain room temperature and poured into ice-cold water to form a colorless solid that afterward was filtered off under a vacuum to afford the desired product. ¹H NMR (400 MHz, CDCl₃, ppm) δ 6.97–6.95 (d, *J* = 8.1 Hz, 1H), 6.95 (s, 1H), 6.83–6.79 (d, *J* = 18.2 Hz, 1H), 5.92–5.89 (d, *J* = 16.2 Hz, 1H), 5.07 (brs, 1H), 4.73 (s, 2H), 4.67 (s, 1H), 4.40–4.39 (d, *J* = 5.5 Hz, 1H), 4.37–4.36 (d, *J* = 5.4 Hz, 2H), 3.84 (s, 3H), 2.50 (s, 1H), 2.33 (s, 1H), 2.24–2.15 (m, 2H), 2.03–1.94 (m, 2H), 1.66 (s, 3H), 1.58 (s, 3H), 1.40–1.33 (m, 1H), 1.24–1.18 (m, 1H), 0.95–0.94 (d, *J* = 8.1 Hz, 3H); IR cm⁻¹: 3280, 3075, 2964, 2924, 2851, 2116, 1638, 1596, 1553, 1513, 1453, 1420, 1378, 1265, 1219, 1140, 1022; exact mass: 343.21, elemental analysis calculated for (C₂₁H₂₉NO₃): C, 73.44; H, 8.51; N, 4.08; O, 13.97; found: C, 73.43; H, 8.54; N, 4.06.

General Procedure of Formation of the 1,2,3-Triazole Ring (18a–o). Same as the General Procedure for Synthesis of the 1,2,3-Triazole Ring (**14a–p**).

(*R*)-(+)-*N*-(3-Methoxy-4-((1-phenyl-1*H*-1,2,3-triazol-4-yl)-methoxy)benzyl)-3,7-dimethyloct-6-enamide (**18a**). Colorless solid, 114.5 mg, 79.3% yield; m.p. = 145.1 °C; ¹H NMR (400 MHz, CDCl₃, ppm) δ 8.81 (s, 1H), 7.74–7.66 (m, 2H), 7.56–7.47 (m, 2H), 7.23–7.14 (m, 1H), 7.11–7.10 (t, *J* = 5.3 Hz, 1H), 6.89–6.88 (d, *J* = 8.1 Hz, 1H), 6.87–6.77 (m, 2H), 5.31 (d, *J* = 8.1 Hz, 2H), 5.08 (m, 1H), 4.38 (d, *J* = 8.1 Hz, 2H), 3.86 (s, 3H), 2.40 (d, *J* = 16.1 Hz, 1H), 2.18 (m, 1H), 2.12–2.01 (m, 1H), 2.01–1.85 (m, 2H), 1.66 (m, 3H), 1.63–1.52 (m, 4H), 1.30 (m, 1H), 0.96 (d, 8.1 Hz, 3H). ¹³C NMR (100 MHz, CDCl₃, ppm) δ 173.9(C=O), 149.4(vanillyl Ar C-OCH₃), 146.8(vanillyl Ar C-OCH₂-), 146.7(triazolyl tertiary C), 136.1(Ar C), 133.2(vanillyl Ar C-CH₂-NH-), 131.1(-CH=C(CH₃)₂), 130.1(Ar C), 127.9(Ar C), 124.1(-CH=C(CH₃)₂), 121.0(vanillyl Ar C), 120.3(triazolyl -CH=C-N-), 119.2(Ar C), 114.8(vanillyl Ar C), 112.0(vanillyl Ar C), 58.1(-OCH₂-), 55.1(-OCH₃), 44.2(-CH₂NH-), 36.4(-COCH₂-),

30.1(-CH₂CH(CH₃)CH₂-), 26.1(-CH₂CHC(CH₃)₂), 24.6(-CH=CHCH₃), 21.6(-CH₂CH₂CHC(CH₃)₂), 21.1(-CH=CHCH₃); IR cm⁻¹: 3313, 3151, 3070, 2960, 2915, 2851, 2366, 1630, 1598, 1572, 1545, 1511, 1457, 1388, 1267, 1220, 1145, 1013; MS (ESI) *m/z*: [M + 1]⁺ 463.25, exact mass: 462.2630, elemental analysis calculated for (C₂₇H₃₄N₄O₃): C, 70.10; H, 7.41; N, 12.11; found: C, 70.13; H, 7.40; N, 12.14.

(*R*)-*N*-(4-((1-(4-Chlorophenyl)-1*H*-1,2,3-triazol-4-yl)methoxy)-3-methoxybenzyl)-3,7-dimethyloct-6-enamide (**18b**). Light yellow solid, 112.3 mg, 77.5% yield; m.p. = 132.5 °C; ¹H NMR (400 MHz, CDCl₃, ppm) δ 8.80 (s, 1H), 7.53–7.47 (m, 2H), 7.35 (d, *J* = 8.1 Hz, 2H), 7.11–7.10 (t, *J* = 5.3 Hz, 1H), 6.89–6.88 (s, 1H), 6.87–6.77 (m, 2H), 5.31 (s, 2H), 5.12–5.04 (brs, 1H), 4.38 (d, *J* = 8.1 Hz, 2H), 3.86 (s, 3H), 2.40 (d, *J* = 16.1 Hz, 1H), 2.18 (d, *J* = 16.1 Hz, 1H), 2.12–2.01 (m, 1H), 2.01–1.85 (m, 2H), 1.66 (m, 3H), 1.63–1.52 (m, 4H), 1.30 (m, 1H), 0.96 (d, *J* = 8.1 Hz, 3H); ¹³C NMR (100 MHz, CDCl₃, ppm) δ 173.93(C=O), 149.6(vanillyl Ar C-OCH₃), 146.6(vanillyl Ar C-OCH₂-), 145.1(triazolyl tertiary C), 134.6(Ar C), 133.2(vanillyl Ar C-CH₂-NH-), 131.3(C=C(CH₃)₂), 129.3(Ar C), 123.9(-CH=C(CH₃)₂), 121.8(Ar C), 121.2(vanillyl Ar C), 120.3(triazolyl -CH=C-N-), 114.2-(vanillyl Ar C), 111.8(vanillyl Ar C), 60.2(-OCH₂-), 56.2(-OCH₃), 45.4(-CH₂NH-), 37.5(-COCH₂-), 31.8(-CH₂CH(CH₃)CH₂-), 25.7(-CH=CHCH₃), 24.1(-CH₂CHC(CH₃)₂), 22.2(-CH=CHCH₃); IR cm⁻¹: 3265, 3144, 3061, 2978, 2958, 2866, 2363, 1665, 1583, 1574, 1540, 1501, 1455, 1386, 1255, 12,359, 1120, 1025; MS (ESI) *m/z*: [M + 1]⁺ 497.22, exact mass: 496.2241, elemental analysis calculated for (C₂₇H₃₃ClN₄O₃): C, 65.25; H, 6.69; N, 11.27; found: C, 65.27; H, 6.70; N, 11.27.

(*R*)-(+)-*N*-(4-((1-(3-Chlorophenyl)-1*H*-1,2,3-triazol-4-yl)methoxy)-3-methoxybenzyl)-3,7-dimethyloct-6-enamide (**18c**). White, 123.3 mg, 85.14% yield; m.p. = 137.0 °C; ¹H NMR (400 MHz, CDCl₃, ppm) δ 8.07 (s, 1H), 7.78 (s, 1H), 7.63–7.61 (d, *J* = 7.9 Hz, 1H), 7.48–7.41 (m, 2H), 7.01–6.99 (d, *J* = 8.1 Hz, 1H), 6.85 (s, 1H), 6.80–6.78 (d, *J* = 8.1 Hz, 1H), 5.67 (brs, 1H), 5.35 (s, 2H), 5.09–5.05 (t, *J* = 7.0 Hz, 1H), 4.39–4.38 (d, *J* = 4.1 Hz, 2H), 3.86 (s, 3H), 2.25–2.21 (q, *J* = 8.1 Hz, 2H), 2.03–1.93 (m, 3H), 1.66 (s, 3H), 1.58 (s, 3H), 1.40–1.18 (m, 2H), 0.96–0.94 (d, 3H); ¹³C NMR (100 MHz, CDCl₃, ppm) δ 171.9(C=O), 149.2(vanillyl Ar C-OCH₃), 146.3(triazolyl tertiary C), 137.3(Ar C), 135.1(Ar C), 132.0(Ar C), 131.1(vanillyl Ar C-CH₂-NH-), 130.4(-CH=C(CH₃)₂), 128.5(Ar C), 123.8(-CH=C(CH₃)₂), 120.3(triazolyl -CH=C-N-), 119.5(Ar C), 118.0(Ar C), 113.6(vanillyl Ar C), 111.1(vanillyl Ar C), 62.8(-OCH₂-), 55.4(-OCH₃), 44.1(-CH₂NH-), 42.8(-COCH₂-), 36.4(-CH₂CH(CH₃)CH₂-), 30.0(-CH₂CH(CH₃)CH₂-), 25.2(-CH₂CHC(CH₃)₂), 25.0(-CH=CHCH₃), 19.1(-CH₂CH₂CHC(CH₃)₂), 17.2(-CH=CHCH₃); IR cm⁻¹: 3311, 3152, 3067, 2957, 2918, 2856, 2361, 1635, 1594, 1578, 1540, 1516, 1456, 1381, 1262, 1229, 1140, 1011; MS (ESI) *m/z*: [M + 1]⁺ 497.50; exact mass: 496.2241; elemental analysis calculated for (C₂₇H₃₃ClN₄O₃): C, 65.25; H, 6.69; Cl, 7.13; N, 11.27; found C, 65.21; H, 6.72; N, 11.26.

(*R*)-(+)-*N*-(4-((1-(2-Chlorophenyl)-1*H*-1,2,3-triazol-4-yl)methoxy)-3-methoxybenzyl)-3,7-dimethyloct-6-enamide (**18d**). White solid, 110.5 mg, 76.30% yield; m.p. = 102.1 °C; ¹H NMR (400 MHz, CDCl₃, ppm) δ 8.06 (s, 1H), 7.62–7.56 (m, 2H), 7.46–7.44 (m, 2H), 7.04 (d, *J* = 8.2 Hz, 1H), 6.84 (s, 1H), 6.81–6.79 (d, *J* = 8.3 Hz, 2H), 5.65 (brs, 1H), 5.37 (s,

2H), 5.09–5.05 (t, *J* = 7.0 Hz, 2H), 4.39–4.38 (d, *J* = 4.4 Hz, 2H), 3.85 (s, 3H), 2.24–2.21 (q, *J* = 8.1 Hz, 2H), 2.03–1.93 (m, 3H), 1.66 (s, 3H), 1.57 (s, 3H), 1.40–1.18 (m, 2H), 0.96–0.94 (d, 3H); ¹³C NMR (100 MHz, CDCl₃, ppm) δ 171.9(C=O), 149.4(vanillyl Ar C-OCH₃), 146.4(vanillyl Ar C-OCH₂-), 143.5(triazolyl tertiary C), 134.3(Ar C), 131.9(Ar C), 131.1(vanillyl Ar C-CH₂-NH-), 130.4(-CH=C(CH₃)₂), 130.3(Ar C), 128.1(Ar C), 127.5(Ar C), 127.3(vanillyl Ar C), 124.7(-CH=C(CH₃)₂), 123.8(triazolyl -CH=C-N-), 119.6(Ar C), 114.1(vanillyl Ar C), 111.2(vanillyl Ar C), 62.8(-OCH₂-), 55.4(-OCH₃), 44.1(-CH₂NH-), 42.8(-COCH₂-), 36.4(-CH₂CH(CH₃)CH₂-), 30.0(-CH₂CH(CH₃)CH₂-), 25.2(-CH₂CHC(CH₃)₂), 25.0(CH=CHCH₃), 19.1(-CH₂CH₂CHC(CH₃)₂), 17.2(CH=CHCH₃); MS (ESI) *m/z*: [M + 1]⁺ 497.50; exact mass: 496.2241; elemental analysis calculated for (C₂₇H₃₃ClN₄O₃): C, 65.25; H, 6.69; Cl, 7.13; N, 11.27; found C, 65.23; H, 6.71; N, 11.25.

(*R*)-(+)-*N*-(4-((1-(2,4-Dichlorophenyl)-1*H*-1,2,3-triazol-4-yl)methoxy)-3-methoxybenzyl)-3,7-dimethyloct-6-enamide (**18e**). White crystalline, 114.6 mg, 74.0% yield; m.p. = 1472.3 °C; ¹H NMR (400 MHz, CDCl₃, ppm) δ 8.37 (s, 1H), 7.87 (d, *J* = 8.1 Hz, 1H), 7.40–7.39 (d, *J* = 8.1 Hz, 1H), 7.30 (s, 1H), 7.11–7.10 (t, *J* = 8.1 Hz, 1H), 6.89–6.87 (d, *J* = 8.1 Hz, 1H), 6.87–6.77 (m, 2H), 5.31 (d, *J* = 8.1 Hz, 2H), 5.12–5.04 (brs, 1H), 4.38–4.37 (d, *J* = 8.1 Hz, 2H), 3.86 (s, 3H), 2.40 (d, *J* = 16.1 Hz, 1H), 2.18 (d, *J* = 16.2 Hz, 1H), 2.12–2.01 (m, 1H), 2.01–1.85 (m, 2H), 1.66 (m, 3H), 1.63–1.52 (m, 4H), 1.30 (m, 1H), 0.96–0.94 (d, *J* = 8.1 Hz, 3H); ¹³C NMR (100 MHz, CDCl₃, ppm) δ 173.3(C=O), 149.0(vanillyl Ar C-OCH₃), 146.4(vanillyl Ar C-OCH₂-), 146.0(triazolyl tertiary C), 134.1(Ar C), 133.5(Ar C), 131.2(vanillyl Ar C-CH₂-NH-), 130.1(-CH=C(CH₃)₂), 129.7(Ar C), 128.0(Ar C), 124.2(-CH=C(CH₃)₂), 122.1(Ar C), 121.2(Ar C), 120.1(triazolyl -CH=C-N-), 114.4(vanillyl Ar C), 112.1(vanillyl Ar C), 59.5(-OCH₂-), 55.7(-OCH₃), 44.0(-CH₂NH-), 36.0(COCH₂-), 30.4(-CH₂CH(CH₃)CH₂-), 26.1(-CH₂CHC(CH₃)₂), 24.9(-CH=CHCH₃), 20.8(-CH₂CH₂CHC(CH₃)₂), 20.5(-CH=CHCH₃); IR cm⁻¹: 3282, 3076, 2954, 2922, 2850, 2360, 1636, 1596, 1553, 1516, 1491, 1491, 1460, 1376, 1265, 1234, 1141, 1044, 1031; LC-MS *m/z*: [M + 1]⁺ 531.50; exact mass: 530.1851; elemental analysis calculated for (C₂₇H₃₂Cl₂N₄O₃): C, 61.02; H, 6.07; Cl, 13.34; N, 10.54; found C, 61.01; H, 6.09; N, 10.55.

(*R*)-(+)-*N*-(4-((1-(3,4-Dichlorophenyl)-1*H*-1,2,3-triazol-4-yl)methoxy)-3-methoxybenzyl)-3,7-dimethyloct-6-enamide (**18f**). White crystalline, 115.6 mg, 74.7% yield; m.p. = 152.5 °C; ¹H NMR (400 MHz, CDCl₃, ppm) δ 8.06 (s, 1H), 7.89 (s, 1H), 7.60 (s, 2H), 7.00–6.98 (d, *J* = 50.4 Hz, 1H), 6.85 (s, 1H), 6.80–6.78 (d, *J* = 7.9 Hz, 1H), 5.72 (brs, 1H), 5.33–5.31 (t, *J* = 8.0 Hz, 2H), 4.38–4.37 (d, *J* = 4.0 Hz, 2H), 3.86 (s, 3H), 2.24–2.21 (q, *J* = 6.0 Hz, 2H), 1.99–1.94 (m, 3H), 1.66 (s, 3H), 1.58 (s, 3H), 1.38–1.18 (m, 2H), 0.95–0.94 (d, *J* = 5.7 Hz, 3H); ¹³C NMR (100 MHz, CDCl₃, ppm) δ 172.5(C=O), 149.8(vanillyl Ar C-OCH₃), 146.8(vanillyl Ar C-OCH₂-), 136.0(Ar C), 134.1(Ar C), 133.1(Ar C), 132.6(Ar C), 131.7(vanillyl Ar C-CH₂-NH-), 131.6(-CH=C(CH₃)₂), 124.4(-CH=C(CH₃)₂), 122.4(Ar C), 121.1(vanillyl Ar C), 120.1(triazolyl -CH=C-N-), 119.5(Ar C), 114.2(vanillyl Ar C), 111.7(vanillyl Ar C), 63.1(-OCH₂-), 56.0(-OCH₃), 44.7(-CH₂NH-), 43.4(-COCH₂-), 37.0(-CH₂CH(CH₃)CH₂-), 30.6(-CH₂CH(CH₃)CH₂-), 25.9(-CH₂CHC(CH₃)₂), 25.5(-CH=CHCH₃), 19.6(-CH₂CH₂CHC(CH₃)₂), 17.8(-CH=CHCH₃); IR cm⁻¹: 3282, 3076, 2954, 2922, 2850,

2360, 1636, 1596, 1553, 1516, 1491, 1491, 1460, 1376, 1265, 1234, 1141, 1044, 1031; LC–MS m/z : $[M+]$ 531.50; exact mass: 530.1851; elemental analysis calculated for $(C_{27}H_{32}Cl_2N_4O_3)$: C, 61.02; H, 6.07; Cl, 13.34; N, 10.54; found C, 61.05; H, 6.06; N, 10.56.

(R)-(+)-N-(3-Methoxy-4-((1-(4-nitrophenyl)-1H-1,2,3-triazol-4-yl)methoxy)benzyl)-3,7-dimethyloct-6-enamide (**18g**). Light yellow solid, 122.8 mg, 83.1%; m.p. = 151.0 °C; 1H NMR (400 MHz, $CDCl_3$, ppm) δ 8.43–8.40 (d, J = 9.2 Hz, 2H), 8.19 (s, 1H), 7.98–7.96 (d, J = 9.0 Hz, 2H), 7.01–6.99 (d, J = 8.1 Hz, 1H), 6.86 (s, 1H), 6.81–6.79 (d, J = 8.1 Hz, 1H), 5.68 (brs, 1H), 5.36 (s, 2H), 5.08–5.05 (t, J = 7.2 Hz, 6.8 Hz, 1H), 4.39–4.38 (d, J = 4.4 Hz, 2H), 3.87 (s, 3H), 2.24–2.21 (m, 2H), 2.03–1.94 (m, 3H), 1.66 (s, 3H), 1.68 (m, 3H), 1.38–1.19 (m, 2H), 0.96–0.94 (d, J = 8.1 Hz, 3H); ^{13}C NMR (100 MHz, $CDCl_3$, ppm) δ 172.5(C=O), 149.8(vanillyl Ar C-OCH₃), 147.4(vanillyl Ar C-OCH₂-), 146.7 (triazolyl tertiary C), 141.1(Ar C), 132.8(Ar C), 131.7(vanillyl Ar C-CH₂-NH-), 125.7(-CH=C(CH₃)₂), 124.4(-CH=C(CH₃)₂), 121.2(Ar C), 120.6(vanillyl Ar C), 120.1(triazolyl -CH=C-N-), 114.2(vanillyl Ar C), 111.7(vanillyl Ar C), 63.1(-OCH₂-), 56.0(-OCH₃), 44.6(-CH₂NH-), 43.3(-COCH₂-), 37.0(-CH₂CH(CH₃)CH₂-), 30.6(-CH₂CH(CH₃)CH₂-), 25.8(-CH₂CHC(CH₃)₂), 25.6(CH=CHCH₃), 19.6(-CH₂CH₂CHC(CH₃)₂), 17.8(CH=CHCH₃); IR cm^{-1} : 3082, 2958, 2850, 1633, 1611, 1565, 1548, 1533, 1464, 1420, 1343, 1266, 1232, 1145, 1090, 1042, 1020, 1005; LC–MS m/z : $[M + 1]^+$ 508.55; HRMS m/z : $[M + 1]^+$ 508.55 exact mass: 507.2482; elemental analysis calculated for $(C_{27}H_{32}Cl_2N_4O_3)$: C, 63.82; H, 6.59; N, 13.88; found C, 63.86; H, 6.57; N, 13.91.

(R)-(+)-N-(3-Methoxy-4-((1-(3-nitrophenyl)-1H-1,2,3-triazol-4-yl)methoxy)benzyl)-3,7-dimethyloct-6-enamide (**18h**). Light yellow solid, 132.1 mg, 89.4%; m.p. = 154.1 °C; 1H NMR (400 MHz, $CDCl_3$, ppm) δ 8.59 (s, 1H), 8.32–8.30 (d, J = 8.2 Hz, 1H), 8.20 (s, 1H), 8.18–8.16 (d, J = 8.1 Hz, 1H), 7.77–7.73 (t, J = 8.0 Hz, 8.0 Hz, 1H), 7.01–6.99 (d, J = 8.1 Hz, 1H), 6.86 (s, 1H), 6.81–6.79 (d, J = 8.4 Hz, 1H), 5.70 (brs, 1H), 5.36 (s, 2H), 5.08–5.05 (t, J = 6.4 Hz, 6.6 Hz, 1H), 4.39–4.38 (d, J = 4.4 Hz, 2H), 3.87 (s, 3H), 2.25–2.21 (d, J = 4.4 Hz, 2H), 2.05–1.94 (m, 3H), 1.66 (s, 3H), 1.58 (s, 3H), 1.40–1.18 (m, 2H), 0.96–0.94 (d, J = 8.1 Hz, 3H); ^{13}C NMR (100 MHz, $CDCl_3$, ppm) δ 172.5(C=O), 149.8(vanillyl Ar C-OCH₃), 149.0(vanillyl Ar C-OCH₂-), 146.8 (triazolyl tertiary C), 137.7(Ar C), 132.7(Ar C), 131.7(vanillyl Ar C-CH₂-NH-), 131.1(Ar C-NO₂), 126.1(-CH=C(CH₃)₂), 124.4(-CH=C(CH₃)₂), 123.4(Ar C), 120.1(triazolyl -CH=C-N-), 115.4(Ar C), 114.2(vanillyl Ar C), 111.7(vanillyl Ar C), 63.1(-OCH₂-), 56.0(-OCH₃), 44.6(-CH₂NH-), 43.4(-COCH₂-), 37.0(-CH₂CH(CH₃)CH₂-), 30.6(-CH₂CH(CH₃)CH₂-), 25.8(-CH₂CHC(CH₃)₂), 25.6(CH=CHCH₃), 19.6(-CH₂CH₂CHC(CH₃)₂), 17.8(CH=CHCH₃); IR cm^{-1} : 3282, 3160, 3077, 2959, 2922, 2872, 1663, 1595, 1522, 1514, 1463, 1349, 1262, 1233, 1160, 1140, 1040; LC–MS m/z : $[M + 1]^+$ 508.55; exact mass: 507.2482; elemental analysis calculated for $(C_{27}H_{32}Cl_2N_4O_3)$: C, 63.89; H, 6.55; N, 13.80; found C, 63.87; H, 6.57; N, 13.78.

(R)-(+)-N-(3-Methoxy-4-((1-(2-nitrophenyl)-1H-1,2,3-triazol-4-yl)methoxy)benzyl)-3,7-dimethyloct-6-enamide (**18i**). Light yellow solid, 135.5 mg, 91.7% yield; m.p. = 86.1 °C; 1H NMR (400 MHz, $CDCl_3$, ppm) δ 8.09–8.07 (d, J = 7.0 Hz, 1H), 7.93 (s, 1H), 7.81–7.79 (t, J = 6.5 Hz, 1H), 7.72–7.68 (t, J = 7.7, 6.8 Hz, 1H), 7.63–7.61 (d, J = 8.1 Hz, 1H), 7.02–7.00 (d, J = 8.1 Hz, 1H), 6.85 (s, 1H), 6.81–6.79 (d, J = 8.2 Hz, 1H), 5.70 (brs, 1H), 5.37 (s, 2H), 5.09–5.05 (t, J = 6.8, 7.1

Hz, 1H), 4.39–4.37 (d, J = 3.9 Hz, 2H), 3.85 (s, 3H), 2.26–2.21 (d, J = 7.9 Hz, 2H), 2.03–1.94 (m, 3H), 1.66 (s, 3H), 1.58 (s, 3H), 1.39–1.18 (m, 2H), 0.96–0.94 (d, J = 8.1 Hz, 3H); ^{13}C NMR (100 MHz, $CDCl_3$, ppm) δ 172.5(C=O), 149.9(vanillyl Ar C-OCH₃), 146.8(vanillyl Ar C-OCH₂-), 145.0(triazolyl tertiary C), 144.5(Ar C-NO₂), 134.0(Ar C), 132.7(Ar C), 131.6(vanillyl Ar C-CH₂-NH-), 131.0(Ar C), 130.3(-CH=C(CH₃)₂), 128.1(vanillyl Ar C), 125.7(Ar C), 124.7(Ar C), 124.4(-CH=C(CH₃)₂), 120.2(triazolyl -CH=C-N-), 114.8(vanillyl Ar C), 111.8(vanillyl Ar C), 63.2(-OCH₂-), 56.0(-OCH₃), 44.6(-CH₂NH-), 43.4(-COCH₂-), 37.0(-CH₂CH(CH₃)CH₂-), 30.6(-CH₂CH(CH₃)CH₂-), 25.8(-CH₂CHC(CH₃)₂), 25.6(CH=CHCH₃), 19.6(-CH₂CH₂CHC(CH₃)₂), 17.8(CH=CHCH₃); IR cm^{-1} : 3082, 2958, 2850, 1633, 1611, 1565, 1548, 1533, 1464, 1420, 1343, 1266, 1232, 1145, 1090, 1042, 1020, 1005; LC–MS m/z : $[M + 1]^+$ 508.55; HRMS m/z : $[M + 1]^+$ 508.55 exact mass: 507.2482; elemental analysis calculated for $(C_{27}H_{32}Cl_2N_4O_3)$: C, 63.82; H, 6.59; N, 13.88; found C, 63.86; H, 6.57; N, 13.91.

(R)-(+)-N-(3-Methoxy-4-((1-(3-(trifluoromethyl)phenyl)-1H-1,2,3-triazol-4-yl)methoxy)benzyl)-3,7-dimethyloct-6-enamide (**18j**). White solid, 126.4 mg, 81.8% yield; m.p. = 162.3 °C; 1H NMR (400 MHz, $CDCl_3$, ppm) δ 8.14 (s, 1H), 8.02 (s, 1H), 7.96–7.94 (d, J = 7.7 Hz, 1H), 7.72–7.65 (m, 2H), 7.02–7.00 (d, J = 8.1 Hz, 1H), 6.86 (s, 1H), 6.81–6.79 (d, J = 8.1 Hz, 1H), 5.67 (brs, 1H), 5.36 (s, 2H), 5.08–5.05 (t, J = 7.0 Hz, 1H), 4.39–4.38 (d, J = 3.9 Hz, 2H), 3.87 (s, 3H), 2.25 (d, J = 7.9 Hz, 2H), 2.03–1.93 (m, 3H), 1.66 (s, 3H), 1.58 (s, 3H), 1.38–1.19 (m, 2H), 0.96–0.94 (d, J = 6.4 Hz, 3H); ^{13}C NMR (100 MHz, $CDCl_3$, ppm) δ 172.5(C=O), 149.8(vanillyl Ar C-OCH₃), 146.8(vanillyl Ar C-OCH₂-), 137.4(triazolyl tertiary C), 132.6(Ar C), 131.7(vanillyl Ar C-CH₂-NH-), 130.7(-CH=C(CH₃)₂), 125.6(Ar C), 125.58(vanillyl Ar C), 124.4(-CH=C(CH₃)₂), 123.7(Ar C), 121.2(Ar C), 120.1(triazolyl -CH=C-N-), 117.6(Ar C), 117.57(Ar C), 114.2(vanillyl Ar C), 111.7(vanillyl Ar C), 63.2(-OCH₂-), 56.0(-OCH₃), 44.7(-CH₂NH-), 43.4(-COCH₂-), 37.0(-CH₂CH(CH₃)CH₂-), 30.6(-CH₂CH(CH₃)CH₂-), 25.8(-CH₂CHC(CH₃)₂), 25.6(CH=CHCH₃), 19.6(-CH₂CH₂CHC(CH₃)₂), 17.8(CH=CHCH₃); LC–MS m/z : $[M + 1]^+$ 531.60; HRMS m/z : $[M + 1]^+$ 531.2582, exact mass: 530.2505; elemental analysis calculated for $(C_{28}H_{33}F_3N_4O_3)$: C, 63.38; H, 6.27; N, 10.56; found C, 63.41; H, 6.28; N, 10.59.

(R)-(+)-N-(4-((1-(4-Fluorophenyl)-1H-1,2,3-triazol-4-yl)-methoxy)-3-methoxybenzyl)-3,7-dimethyloct-6-enamide (**18k**). White solid, 126.4 mg, 81.8% yield; m.p. = 162.3 °C; 1H NMR (400 MHz, $CDCl_3$, ppm) δ 8.81 (s, 1H), 7.62–7.55 (m, 2H), 7.15–7.07 (m, 2H), 6.89 (dt, J = 1.7, 0.8 Hz, 1H), 6.87–6.77 (m, 2H), 5.31–5.32 (d, J = 8.1 Hz, 2H), 5.08 (brs, 1H), 4.38–4.37 (d, J = 8.1 Hz, 2H), 3.86 (s, 3H), 2.40 (d, J = 16.1 Hz, 1H), 2.18 (d, J = 16.2 Hz, 1H), 2.12–2.01 (m, 1H), 2.01–1.85 (m, 2H), 1.66 (m, 3H), 1.63–1.52 (m, 2H), 1.30 (m, 1H), 0.96 (d, J = 8.1 Hz, 3H); ^{13}C NMR (100 MHz, $CDCl_3$, ppm) δ 172.5(C=O), 165.1(Ar C-F), 163.3(Ar C), 148.4(vanillyl Ar C-OCH₃), 147.5(triazolyl tertiary C), 146.1(vanillyl Ar C-OCH₂-), 133.8(Ar C), 132.1(vanillyl Ar C-CH₂-NH-), 131.4(-CH=C(CH₃)₂), 124.3(-CH=C(CH₃)₂), 122.9(Ar C), 121.5(triazolyl -CH=C-N-), 119.9(Ar C), 117.2(Ar C), 117.11(vanillyl Ar C), 114.6(vanillyl Ar C), 112.2(vanillyl Ar C), 59.1(-OCH₂-), 55.8(-OCH₃), 44.2(-CH₂NH-), 36.2(-COCH₂-), 30.1(-CH₂CH(CH₃)CH₂-), 26.1(-CH₂CHC(CH₃)₂), 24.6(CH=CHCH₃), 20.6(-CH₂CH₂CHC(CH₃)₂), 20.17(CH=CHCH₃); IR cm^{-1} : 3325,

3122, 3075, 2969, 2904, 2841, 2365, 1639, 1595, 1569, 1533, 1505, 1447, 1393, 1261, 1214, 1145, 1010; MS (ESI) m/z : $[M + 1]^+$ 481.26; exact mass: 480.2536; elemental analysis calculated for $(C_{28}H_{33}F_3N_4O_3)$: C, 63.38; H, 6.27; N, 10.56; found C, 63.41, H, 6.28; N, 10.59.

(*R*)-(+)-*N*-4-((1-(2-Fluorophenyl)-1*H*-1,2,3-triazol-4-yl)methoxy)-3-methoxybenzyl)-3,7-dimethyloct-6-enamide (**18l**). Pale yellow solid, 111.9 mg, 80.0% yield; m.p. = 119.1 °C; 1H NMR (400 MHz, $CDCl_3$, ppm) δ 8.18 (s, 1H), 7.96–7.93 (t, J = 7.4 Hz, 1H), 7.46–7.29 (m, 3H), 7.04–7.02 (d, J = 8.2 Hz, 1H), 6.84 (s, 1H), 6.80–6.78 (d, J = 8.1 Hz, 1H), 5.68 (brs, 1H), 5.36 (s, 2H), 5.07–5.05 (t, J = 6.7 Hz, 1H), 4.38–4.37 (d, J = 4.6 Hz, 2H), 3.85 (s, 3H), 2.25–2.21 (dd, J = 8.4 Hz, 2H), 2.01–1.93 (m, 3H), 1.66 (s, 3H), 1.58 (s, 3H), 1.42–1.18 (m, 2H), 0.95–0.94 (d, J = 6.1 Hz, 3H); ^{13}C NMR (100 MHz, $CDCl_3$, ppm) δ 172.5(C=O), 154.7(Ar C-F), 152.2-(triazolyl tertiary C), 149.9(vanillyl Ar C-OCH₃), 146.9-(vanillyl Ar C-OCH₂-), 132.5(Ar C), 131.6(vanillyl Ar C-CH₂-NH-), 130.5(Ar C), 130.4(-CH=C(CH₃)₂), 125.4-(vanillyl Ar C), 125.3(Ar C), 125.2(Ar C), 124.9(Ar C), 124.4(-CH=C(CH₃)₂), 120.1(triazolyl -CH=C-N-), 117.2(Ar C), 117.0(Ar C), 114.5(vanillyl Ar C), 111.7(vanillyl Ar C), 63.2(OCH₂), 55.9(-OCH₃), 44.6(-CH₂NH-), 43.4(-COCH₂-), 37.0(-CH₂CH(CH₃)CH₂-), 30.6(-CH₂CH(CH₃)CH₂-), 25.8(-CH₂CHC(CH₃)₂), 25.5(CH=CHCH₃), 19.6(-CH₂CH₂CHC(CH₃)₂), 17.7(CH=CHCH₃); IR cm^{-1} : 3453, 3289, 3147, 3065, 2965, 2916, 2873, 2362, 1636, 1598, 1545, 1516, 1465, 1378, 1261, 1234, 1163, 1135, 1040; LC-MS m/z : $[M + 1]^+$ 481.25; exact mass: 480.2537; elemental analysis calculated for $(C_{27}H_{33}FN_4O_3)$: C, 67.48; H, 6.92; N, 11.66; found C, 67.47; H, 6.95; N, 11.65.

(*R*)-(+)-*N*-4-((1-(4-Cyanophenyl)-1*H*-1,2,3-triazol-4-yl)methoxy)-3-methoxybenzyl)-3,7-dimethyloct-6-enamide (**18m**). White solid, 108.5 mg, 76.4% yield; m.p. = 140.0 °C, 1H NMR (400 MHz, $CDCl_3$, ppm) δ 8.16 (s, 1H), 7.92–7.90 (d, J = 8.6 Hz, 1H), 7.84–7.82 (d, J = 8.5 Hz, 2H), 7.00–6.98 (d, J = 8.2 Hz, 1H), 6.85 (s, 1H), 6.80–6.78 (d, J = 8.1 Hz, 1H), 5.75 (brs, 1H), 5.34 (s, 2H), 5.08–5.05 (t, J = 6.9 Hz, 1H), 4.39–4.37 (d, J = 4.4 Hz, 2H), 3.86 (s, 3H), 2.25–2.21 (d, J = 8.4 Hz, 2H), 2.04–1.94 (m, 3H), 1.70 (s, 3H), 1.58 (s, 3H), 1.38–1.18 (m, 2H), 0.96–0.94 (d, J = 6.4 Hz, 3H); ^{13}C NMR (100 MHz, $CDCl_3$, ppm) δ 172.6(C=O), 149.8(vanillyl Ar C-OCH₃), 146.7(vanillyl Ar C-OCH₂-), 145.9(triazolyl tertiary C), 139.8(Ar C), 134.0(Ar C), 132.7(vanillyl Ar C-CH₂-NH-), 131.7(-CH=C(CH₃)₂), 124.3(-CH=C(CH₃)₂), 121.0(vanillyl Ar C), 120.7(Ar C), 120.0(triazolyl -CH=C-N-), 117.8(Ar-CN), 114.2(vanillyl Ar C), 112.6(Ar C), 111.6(vanillyl Ar C), 63.0(-OCH₂-), 56.0(-OCH₃), 44.6(-CH₂NH-), 43.3(-COCH₂-), 37.0(-CH₂CH(CH₃)CH₂-), 30.6(-CH₂CH(CH₃)CH₂-), 25.8(-CH₂CHC(CH₃)₂), 25.5(CH=CHCH₃), 19.6(-CH₂CH₂CHC(CH₃)₂), 17.7(CH=CHCH₃); IR cm^{-1} : 3280, 3068, 2918, 2873, 1639, 1595, 1557, 1516, 1454, 1377, 1321, 1266, 1234, 1220, 1137, 1044; LC-MS m/z : $[M + 1]^+$ 488.25; exact mass: 487.2583; elemental analysis calculated for $(C_{28}H_{33}N_5O_3)$: C, 68.97; H, 6.82; N, 14.36; found C, 68.99; H, 6.84; N, 14.39.

(*R*)-(+)-*N*-4-((1-(4-Bromophenyl)-1*H*-1,2,3-triazol-4-yl)methoxy)-3-methoxybenzyl)-3,7-dimethyloct-6-enamide (**18n**). White solid, 116.8 mg, 74.0% yield; m.p. = 154.7 °C; 1H NMR (400 MHz, $CDCl_3$, ppm) δ 8.05 (s, 1H), 7.66–7.60 (d, J = 12.8 Hz, 4H), 7.02–7.00 (d, J = 8.1 Hz, 1H), 6.85 (s, 1H), 6.80–6.78 (d, J = 8.2 Hz, 1H), 5.66 (brs, 1H), 5.34 (s, 2H), 5.08–5.04 (t, J = 6.9 Hz, 1H), 4.38–4.37 (d, J = 4.2 Hz, 2H),

3.86 (s, 3H), 2.24–2.20 (d, J = 6.3 Hz, 2H), 2.03–1.93 (m, 3H), 1.66 (s, 3H), 1.58 (m, 3H), 1.38–1.18 (m, 2H), 0.95–0.94 (d, J = 8.1 Hz, 3H); ^{13}C NMR (100 MHz, $CDCl_3$, ppm) δ 172.5(C=O), 149.8(vanillyl Ar C-OCH₃), 146.8(vanillyl Ar C-OCH₂-), 145.4(triazolyl tertiary C), 136.0(Ar C), 133.1(Ar C), 132.5(vanillyl Ar C-CH₂-NH-), 131.7(-CH=C(CH₃)₂), 124.4(-CH=C(CH₃)₂), 122.7(Ar C-Br), 122.0(Ar C), 121.1-(vanillyl Ar C), 120.1(triazolyl -CH=C-N-), 114.2(vanillyl Ar C), 111.7(vanillyl Ar C), 63.1(-OCH₂), 56.0(-OCH₃), 44.7(-CH₂NH-), 43.4, 37.0(-COCH₂-), 30.6(-CH₂CH(CH₃)CH₂-), 25.8(-CH₂CHC(CH₃)₂), 25.6(CH=CHCH₃), 19.7(-CH₂CH₂CHC(CH₃)₂), 17.8(CH=CHCH₃); IR cm^{-1} : 3277, 3174, 3068, 2949, 2918, 2846, 2360, 1640, 1595, 1553, 1468, 1451, 1265, 1235, 1137, 1044, 1044, 1031, 1021; LC-MS m/z : $[M + 3]^+$ 543.50; exact mass: 540.1736; elemental analysis calculated for $(C_{27}H_{33}BrN_4O_3)$: C, 59.89; H, 6.14; N, 10.35; found C, 59.93; H, 6.11; N, 10.32.

(*R*)-(+)-*N*-4-((1-(3,4-Dimethylphenyl)-1*H*-1,2,3-triazol-4-yl)methoxy)-3-methoxybenzyl)-3,7-dimethyloct-6-enamide (**18o**). White solid, 130.2 mg, 91.1% yield; m.p. = 91.3 °C; 1H NMR (400 MHz, $CDCl_3$, ppm) δ 8.03 (s, 1H), 7.50 (s, 1H), 7.40–7.38 (d, J = 7.9 Hz, 1H), 7.23 (s, 1H), 7.03–7.01 (d, J = 8.3 Hz, 1H), 6.84 (s, 1H), 6.80–6.78 (d, J = 8.2 Hz, 1H), 5.71 (brs, 1H), 5.33 (s, 2H), 5.08–5.05 (t, J = 6.9 Hz, 1H), 4.38–4.37 (d, J = 4.2 Hz, 2H), 3.85 (s, 3H), 2.33 (s, 3H), 2.31 (s, 3H), 2.25–2.20 (d, J = 16.3 Hz, 1H), 2.03–1.93 (m, 3H), 1.66 (s, 3H), 1.58 (s, 3H), 1.38–1.19 (m, 2H), 0.95–0.94 (d, J = 8.1 Hz, 3H); ^{13}C NMR (100 MHz, $CDCl_3$, ppm) δ 172.5(C=O), 149.8(vanillyl Ar C-OCH₃), 146.9(vanillyl Ar C-OCH₂-), 138.5(triazolyl tertiary C), 137.8(Ar C), 134.9(Ar C), 132.4(Ar C), 131.6(vanillyl Ar C-CH₂-NH-), 130.7(-CH=C(CH₃)₂), 124.4(-CH=C(CH₃)₂), 121.8(vanillyl Ar C), 120.2(triazolyl -CH=C-N-), 117.9(Ar C), 114.2(vanillyl Ar C), 111.7(vanillyl Ar C), 63.3(-OCH₂), 55.9(-OCH₃), 44.6(-CH₂NH-), 43.4(-COCH₂-), 37.0(Ar CCH₃), 30.6(-CH₂CH(CH₃)CH₂-), 25.8(-CH₂CHC(CH₃)₂), 25.6, 20.0(CH=CHCH₃), 19.64(Ar CH₃), 19.58(-CH₂CH₂CHC(CH₃)₂), 17.8(CH=CHCH₃); IR cm^{-1} : 3287, 2957, 2916, 2799, 2361, 1634, 1595, 1514, 1461, 1261, 1136, 1041; LC-MS m/z : $[M + 1]^+$ 491.60; exact mass: 490.2944; elemental analysis calculated for $(C_{29}H_{38}N_4O_3)$: C, 70.99; H, 7.81; N, 11.42; found C, 70.95; H, 7.84; N, 11.46.

Biological Assays. In Vitro Antiproliferative Activity at a Single Dose. All the synthesized compounds were screened for their antiproliferative activity against a panel of 60 cancer cell lines at the National Cancer Institute, Bethesda, MD, USA, as per the standard procedure given at <http://www.dtp.nci.nih.gov>. The RPMI 1640 medium (5% fetal bovine serum and 2 mM L-glutamine) was used to grow the human tumor cell lines. All the tumor cells were incubated into a 96-well microtiter plate. Then this plate was placed for incubation at 37 °C for 24 h. After those two plates of each cell line were fixed with TCA *in situ*, and optical density was measured at this point, which represented the cell population of each cell line at the time of compound addition (OD_{zero}). On the other hand, all the tested compounds were dissolved in DMSO to yield 400-fold desired final concentration and stored at –80 °C. These frozen compounds were thawed, and their aliquot part was diluted to 10^{–4} M concentration with the medium containing 50 μ g/mL of gentamicin at the time of compound addition. The control sample was made with DMSO only. The tested compounds (100 μ L) from the aliquot parts were added to the appropriate 96-well microtiter plate containing 100 μ L

of the medium resulting in the required final drug concentrations of 10^{-5} and 0 M (control). After the addition of tested compounds, the 96-well microtiter plate was incubated for 48 h at 100%, 5% CO_2 , 95% air, and 100% relative humidity. Cold TCA was used to stop the assay for adherent cells. Further on, 50 mL of 50% (w/v) TCA was used to fix the cell and incubated for 1 h at 4 °C. The supernatant was removed, and the 96-well microtiter plates were rinsed five times with water and air dried. A 100 mL solution of the protein binding dye Sulforhodamine B (SRB) was made at 0.4% (w/v) in 1% acetic acid and added to each well of the plates. These plates were placed at room temperature for incubation for 10 min and then washed with 1% acetic acid five times to remove unbound dye. Then the plates were treated with 10 mM Trizma base so that unbound dye was solubilized with the Trizma base. The absorbance was measured at a wavelength of 515 nm on an automated plate reader, and results for each tested compound were calculated as the percent of tumor growth of the treated cells in comparison with the untreated control cells. Optical density (OD) was recorded for the SRB-derived color just before exposing the cells to the test compound (OD_{zero}) and after 48 h exposure to the test compound (OD_{test}) or the control vehicle (OD_{ctrl}).

Cell Lines, Cell Culture, Growth Conditions, and Reagents. A panel of human cancer cell lines, namely, MCF-7 (breast), NCI-H460, A549 (lung), MiaPaCa (pancreas), HCT-116 (colon), and PC-3 (prostate), was purchased from ATCC. The cell lines were grown in T75 tissue culture flasks in a complete growth medium (RPMI-1640 and DMEM) added with 10% FBS, 100 mg/mL streptomycin, as well as 100 U/mL penicillin in a humidified carbon dioxide incubator (New Brunswick, Galaxy 170R, Eppendorf) at 37 °C and 5% CO_2 with 95% relative humidity. DAPI (4',6'-diamidino-2-phenylindole) and Rhodamine-123, DCFDA (2',7'-dichlorofluorescein diacetate) were procured from Sigma-Aldrich (St. Louis, MO, USA). Sulforhodamine B dye was purchased from Hi Media. Monolayer cultures of the above cell lines were trypsinized using 0.25% trypsin/EDTA (1 mM) solution. After the cells got detached, the activity of trypsin/EDTA solution was stopped using the complete growth medium and centrifuged at 900 rpm for 5 min. Cells were again dispersed in the complete growth medium in tissue culture flasks and incubated in a CO_2 incubator. When cells attained approx. 50–60% confluency, they were treated with target compounds dissolved in DMSO and the untreated control cultures with DMSO (<0.2%).

Cytotoxicity Activity against Different Cancer Cell Lines. The *in vitro* cytotoxicity activity of target compounds (18a–o) was carried out using the SRB (Sulforhodamine B) assay method reported. For preliminary screening, optimum inoculum densities per well of A549, NCI-H460, MCF-7, and HCT-116 cell lines were seeded in 96-well flat-bottom plates (NUNC). Briefly, 100 mL/well of cell suspensions was seeded in 96-well tissue culture plates and incubated for 24 h. When cells attained 50–60% confluency, then different concentrations of anticancer test compounds were incubated and kept for another 48 h. Next, after the completion of 48 h incubation, the cells were settled using 50% ice-cold trichloroacetic acid (TCA) and kept at 4 °C for 1 h, and the plates were washed thrice in an aqueous medium and air dried. Once the plates dried, 100 mL/well SRB dye was added and kept for half an hour at room temperature. Soon after, the plates were again washed thrice using 1% glacial acetic acid to eliminate excess

unbound SRB, and the plates were further air dried. When the plates were completely dried, the bound SRB was solubilized by adding 100 mL/well 10 mM TRIS (tris(hydroxymethyl)aminomethane) buffer at pH 10.5, and plates were kept on an orbital shaker for 5 min. Lastly, absorbance was recorded at 540 nm in a microplate reader (Tecan Infinite M Nano). IC_{50} was determined by GraphPad Prism 6.⁵⁵

Reactive Oxygen Species (ROS) Generation Assay. Dye 2',7'-dichlorofluorescein diacetate (DCFH-DA) was used to measure intracellular ROS production. DCFH gets transformed into highly fluorescent 2',7'-dichlorofluorescein (DCF) in the presence of an oxidant. In this study, 1×10^5 A549 cells were incubated for 24 h in six-well plates and 1.5, 3, and 5 μM concentration of molecule 18f and kept for a further 48 h incubation. H_2O_2 (0.05%) was used as the standard positive control and added 1 h before conclusion of the experiment. The cells were washed with ice-cold PBS, and 10 mM DCFH-DA was added to all the wells for 30 min in the dark. The plate was further washed with cold PBS, and the final volume of incomplete media was added to each well and finally observed under an inverted fluorescence microscope (Olympus IX70).^{56,57}

Apoptosis Assay through DAPI Staining. To examine apoptotic cell death qualitatively, morphological variations in chromatin structure were detected using DAPI staining. Precisely, A549 cells at a density of 1×10^5 were seeded in six-well tissue culture plates and kept for 24 h to attain confluency of about 50–60%, treatment was given to the plate with the above-mentioned concentration of compound 18f and paclitaxel used as standard positive control drug, and cells were kept for 48 h incubation. Later, cells were washed with ice-cold PBS to remove dead cell moieties. Again, cells were fixed using 70% ethanol for 1 h at room temperature and washed with cold PBS. Finally, the cells were stained with 1 mg/mL DAPI in the dark for 5 min and washed with ice-cold PBS, the final volume of PBS was added to each well, and the plate was observed under an inverted fluorescence microscope (Olympus IX70).⁵⁸

Measurement of the Loss of Mitochondrial Membrane Potential ($\Delta\Psi\text{m}$). Mitochondrial perturbation due to the loss of membrane potential was studied using dye rhodamine-123 by a fluorescence microscope qualitatively. Non-small lung cancer A549 cells (1×10^5 /mL/well) were seeded in six-well tissue culture plates; treated with 1.5, 3.0, and 5.0 μM concentration of compound 18f and paclitaxel used as the standard positive control drug; and incubated for 48 h. After treatment, cells were washed with ice-cold PBS; later, the final concentration of 0.2 mM rhodamine was incubated to all the wells and finally kept for 20–30 min in the dark inside the incubator. Further, cells were washed with cold PBS, and the final volume of incomplete media was added to all the wells and analyzed under a fluorescence microscope (Olympus IX70).⁵⁹

Cell Cycle Analysis. A549 cancer cells were treated with compound 18f and analyzed for the distribution of cell population in different phases of the cell cycle. After 48 h of treatment, the cells were harvested and washed with phosphate buffer saline (PBS). The cells were then fixed with ice-cold 70% ethanol. After overnight incubation at 4 °C, the cells were washed with PBS and incubated with propidium iodide solution (20 $\mu\text{g}/\text{mL}$) containing RNase (10 $\mu\text{g}/\text{mL}$) at 37 °C for half an hour. The cells were analyzed using a BD FACSverse cytometer. A total of 10,000 events were analyzed

for each sample, and the data were analyzed using the Modfit LT software.²³

Wound Healing Assay. A549 cells (4×10^5) were seeded and grown within six-well plates until a monolayer was formed. Then, by using a 200 μ L pipette tip, a scratch was given in the confluent monolayer. Cells were washed with $1 \times$ PBS to remove detached cells before incubating with fresh media with different compound **18f** concentrations (3, 10, and 30 μ M) or DMSO vehicle control. Cell migration across the wound area was captured at two time intervals (0 and 24 h) with an inverted microscope. The wound area was measured using the ImageJ software, and the percentage wound healed area during the course of the assay was calculated after normalizing the wound area.²³

■ ASSOCIATED CONTENT

SI Supporting Information

The Supporting Information is available free of charge at <https://pubs.acs.org/doi/10.1021/acsomega.2c03325>.

Dose–response curve, toxicity of most potent compound **18f**, migration capacities (NCI-H460), colony-forming ability (NCI-H460), ¹H NMR, ¹³C NMR, and mass spectral data of synthesized compounds were incorporated (PDF)

■ AUTHOR INFORMATION

Corresponding Authors

Gousia Chashoo – Pharmacology Division, CSIR-Indian Institute of Integrative Medicine, Jammu 180001, India; Email: syedshafi@jamiyahamdard.ac.in

Syed Shafi – Department of Chemistry, School of Chemical and Life Sciences, Jamia Hamdard, New Delhi 110062, India; orcid.org/0000-0001-7657-0630; Email: chashoo.gousia@gmail.com

Authors

Arif Khan – Department of Chemistry, School of Chemical and Life Sciences, Jamia Hamdard, New Delhi 110062, India

Fatima Naaz – Department of Chemistry, School of Chemical and Life Sciences, Jamia Hamdard, New Delhi 110062, India

Rafia Basit – Pharmacology Division, CSIR-Indian Institute of Integrative Medicine, Jammu 180001, India

Deepak Das – Department of Chemistry, School of Chemical and Life Sciences, Jamia Hamdard, New Delhi 110062, India

Piyush Bisht – Faculty of Life Sciences and Biology, South Asian University, New Delhi 110021, India

Majeed Shaikh – Natural product and Medicinal Chemistry Division, CSIR-Indian Institute of Integrative Medicine, Jammu 180001, India

Bilal Ahmad Lone – Faculty of Life Sciences and Biology, South Asian University, New Delhi 110021, India

Yuba Raj Pokharel – Faculty of Life Sciences and Biology, South Asian University, New Delhi 110021, India

Qazi Naveed Ahmed – Natural product and Medicinal Chemistry Division, CSIR-Indian Institute of Integrative Medicine, Jammu 180001, India; orcid.org/0000-0002-6890-7587

Shazia Parveen – Faculty of Science, Chemistry Department, Taibah University, Yanbu 46423, Saudi Arabia; orcid.org/0000-0002-2213-2958

Intzar Ali – Department of Microbiology, Hamdard Institute of Medical Sciences and Research, Jamia Hamdard, New Delhi 110062, India

Shashank Kumar Singh – Pharmacology Division, CSIR-Indian Institute of Integrative Medicine, Jammu 180001, India

Complete contact information is available at:

<https://pubs.acs.org/10.1021/acsomega.2c03325>

Notes

The authors declare no competing financial interest.

■ ACKNOWLEDGMENTS

We thankfully acknowledge the technical and analytical support by DIF Chemistry-Jamia Hamdard and CIF-Jamia Hamdard. A.K. would like to thank CSIR New Delhi for providing fellowship under. 09/591(0148)/2017-EMR-1. S.S. is grateful to DST for providing project under DST-SERB-ECR/2017/001067/CS.

■ REFERENCES

- (1) Hirsch, F. R.; Scagliotti, G. V.; Mulshine, J. L.; Kwon, R.; Curran, W. J., Jr.; Wu, Y.-L.; Paz-Ares, L. Lung Cancer: Current Therapies and New Targeted Treatments. *Lancet* **2017**, *389*, 299–311.
- (2) Kuo, T.-C.; Li, L.-W.; Pan, S.-H.; Fang, J.-M.; Liu, J.-H.; Cheng, T.-J.; Wang, C.-J.; Hung, P.-F.; Chen, H.-Y.; Hong, T.-M.; Hsu, Y.-L.; Wong, C.-H.; Yang, P.-C. Purine-Type Compounds Induce Microtubule Fragmentation and Lung Cancer Cell Death through Interaction with Katanin. *J. Med. Chem.* **2016**, *59*, 8521–8534.
- (3) Hou, H.; Qu, B.; Su, C.; Hou, G.; Gao, F. Design, Synthesis and Anti-Lung Cancer Evaluation of 1, 2, 3-Triazole Tethered Dihydroartemisinin-Isatin Hybrids. *Front. Pharmacol.* **2021**, *12*, DOI: 10.3389/fphar.2021.801580.
- (4) Sławiński, G.; Wrona, A.; Dąbrowska-Kugacka, A.; Raczak, G.; Lewicka, E. Immune Checkpoint Inhibitors and Cardiac Toxicity in Patients Treated for Non-Small Lung Cancer: A Review. *Int. J. Mol. Sci.* **2020**, *21*, 7195.
- (5) Jun, J. J.; Duscharla, D.; Ummanni, R.; Hanson, P. R.; Malhotra, S. V. Investigation on the Anticancer Activity of Symmetric and Unsymmetric Cyclic Sulfamides. *ACS Med. Chem. Lett.* **2021**, *12*, 202–210.
- (6) Meng, Y.; Yu, B.; Huang, H.; Peng, Y.; Li, E.; Yao, Y.; Song, C.; Yu, W.; Zhu, K.; Wang, K.; Yi, D.; Du, J.; Chang, J. Discovery of Dosimertinib, a Highly Potent, Selective, and Orally Efficacious Deuterated EGFR Targeting Clinical Candidate for the Treatment of Non-Small-Cell Lung Cancer. *J. Med. Chem.* **2021**, *64*, 925–937.
- (7) Arcaro, A.; Fischer, B. Current Status of Clinical Trials for Small Cell Lung Cancer. *Rev. Recent Clin. Trials* **2008**, *3*, 40–61.
- (8) Kauffmann-Guerrero, D.; Tufman, A. Rare Driver Alterations in Nonsmall Cell Lung Cancer: Novel Targeted Drugs. *Curr. Opin. Oncol.* **2022**, *34*, 77–82.
- (9) Sankar, K.; Bryant, A. K.; Strohbahn, G. W.; Zhao, L.; Elliott, D.; Moghanaki, D.; Kelley, M. J.; Ramnath, N.; Green, M. D. Real World Outcomes versus Clinical Trial Results of Durvalumab Maintenance in Veterans with Stage III Non-Small Cell Lung Cancer. *Cancers* **2022**, *14*, 614.
- (10) Szumilak, M.; Wiktorowska-Owczarek, A.; Stanczak, A. Hybrid Drugs—A Strategy for Overcoming Anticancer Drug Resistance? *Molecules* **2021**, *26*, 2601.
- (11) Naaz, F.; Haider, M. R.; Shafi, S.; Yar, M. S. Anti-Tubulin Agents of Natural Origin: Targeting Taxol, Vinca, and Colchicine Binding Domains. *Eur. J. Med. Chem.* **2019**, *171*, 310–331.
- (12) Lichota, A.; Gwozdziński, K. Anticancer Activity of Natural Compounds from Plant and Marine Environment. *Int. J. Mol. Sci.* **2018**, *19*, 3533.

- (13) Shahzadi, I.; Zahoor, A. F.; Rasul, A.; Mansha, A.; Ahmad, S.; Raza, Z. Synthesis, Hemolytic Studies, and In Silico Modeling of Novel Acefylline-1,2,4-Triazole Hybrids as Potential Anti-Cancer Agents against MCF-7 and A549. *ACS Omega* **2021**, *6*, 11943–11953.
- (14) Jaganathan, R.; Purushotham, B.; Radhakrishnan, N.; Swamy, M. K. Capsaicin and Its Potential Anticancer Mechanisms of Action. *Plant-derived Bioact. Chem. Mode Action* **2020**, 301–321.
- (15) Walpole, C. S. J.; Wrigglesworth, R.; Bevan, S.; Campbell, E. A.; Dray, A.; James, I. F.; Masdin, K. J.; Perkins, M. N.; Winter, J. Analogues of Capsaicin with Agonist Activity as Novel Analgesic Agents; Structure—Activity Studies. 2. The Amide Bond “B-Region.”. *J. Med. Chem.* **1993**, *36*, 2373–2380.
- (16) Naaz, F.; Khan, A.; Kumari, A.; Ali, I.; Ahmad, F.; Ahmad Lone, B.; Ahmad, N.; Ali Khan, I.; Rajput, V. S.; Grover, A.; Shafi, S. 1,3,4-Oxadiazole Conjugates of Capsaicin as Potent NorA Efflux Pump Inhibitors of *Staphylococcus Aureus*. *Bioorg. Chem.* **2021**, *113*, No. 105031.
- (17) Uarota, V. G.; Maraschin, M.; de Bairros, Â. D. F. M.; Pedreschi, R. Factors Affecting the Capsaicinoid Profile of Hot Peppers and Biological Activity of Their Non-Pungent Analogs (Capsinoids) Present in Sweet Peppers. *Crit. Rev. Food Sci. Nutr.* **2021**, *61*, 1–17.
- (18) Jun, H.-S.; Park, T.; Lee, C. K.; Kang, M. K.; Park, M. S.; Kang, H. I.; Surh, Y.-J.; Kim, O. H. Capsaicin Induced Apoptosis of B16-F10 Melanoma Cells through down-Regulation of Bcl-2. *Food Chem. Toxicol.* **2007**, *45*, 708–715.
- (19) Narang, N.; Jiraungkoorskul, W.; Jamrus, P. Current Understanding of Antiobesity Property of Capsaicin. *Pharmacogn. Rev.* **2017**, *11*, 23.
- (20) Richbart, S. D.; Friedman, J. R.; Brown, K. C.; Gadepalli, R. S.; Miles, S. L.; Rimoldi, J. M.; Rankin, G. O.; Valentovic, M. A.; Tirona, M. T.; Finch, P. T.; Hess, J. A.; Dasgupta, P. Nonpungent N-AVAM Capsaicin Analogues and Cancer Therapy. *J. Med. Chem.* **2021**, *64*, 1346–1361.
- (21) Wang, Y.; Zhou, Y.; Fu, J. Advances in Antiobesity Mechanisms of Capsaicin. *Curr. Opin. Pharmacol.* **2021**, *61*, 1–5.
- (22) Naaz, F.; Ahmad, F.; Lone, B. A.; Pokharel, Y. R.; Fuloria, N. K.; Fuloria, S.; Ravichandran, M.; Pattabhiraman, L.; Shafi, S.; Shahar Yar, M. Design and Synthesis of Newer 1,3,4-Oxadiazole and 1,2,4-Triazole Based Toposentin Analogues as Anti-Proliferative Agent Targeting Tubulin. *Bioorg. Chem.* **2020**, *95*, No. 103519.
- (23) Naaz, F.; Ahmad, F.; Lone, B. A.; Khan, A.; Sharma, K.; IntzarAli; ShaharYar, M.; Pokharel, Y. R.; Shafi, S. Apoptosis Inducing 1,3,4-Oxadiazole Conjugates of Capsaicin: Their In Vitro Anti-proliferative and In Silico Studies. *ACS Med. Chem. Lett.* **2021**, *12*, 1694–1702.
- (24) Chapa-oliver, A. M.; Mejia-teniente, L.; Chili, K. Capsaicin : From ePlants to a Cancer-Suppressing Agent. 2016, 1–14, DOI: 10.3390/molecules21080931.
- (25) Friedman, J. R.; Richbart, S. D.; Merritt, J. C.; Brown, K. C.; Denning, K. L.; Tirona, M. T.; Valentovic, M. A.; Miles, S. L.; Dasgupta, P. Capsaicinoids: Multiple Effects on Angiogenesis, Invasion and Metastasis in Human Cancers. *Biomed. Pharmacother.* **2019**, *118*, No. 109317.
- (26) YANG, J.; LI, T. Z.; XU, G. H.; LUO, B. B.; CHEN, Y. X.; ZHANG, T. Low-Concentration Capsaicin Promotes Colorectal Cancer Metastasis by Triggering ROS Production and Modulating Akt/MTOR and STAT-3 Pathways. *Neoplasma* **2013**, *60*, 364–372.
- (27) Surh, Y.-J.; Lee, S. S. Capsaicin in Hot Chili Pepper: Carcinogen, Co-Carcinogen or Anticarcinogen? *Food Chem. Toxicol.* **1996**, *34*, 313–316.
- (28) Liao, J.-C.; Deng, J.-S.; Lin, Y.-C.; Lee, C.-Y.; Lee, M.-M.; Hou, W.-C.; Huang, S.-S.; Huang, G.-J. Antioxidant, Antinociceptive, and Anti-Inflammatory Activities from *Actinidia Callosa* Var. *Callosa* In Vitro and In Vivo. *Evidence-Based Complementary Altern. Med.* **2012**, *2012*, 1–14.
- (29) Kamarudin, N.; Hisamuddin, N.; Ong, H.; Ahmad Azmi, A.; Leong, S.; Abas, F.; Sulaiman, M.; Shaik Mossadeq, W. Analgesic Effect of 5-(3,4-Dihydroxyphenyl)-3-Hydroxy-1-(2-Hydroxyphenyl)-Penta-2,4-Dien-1-One in Experimental Animal Models of Nociception. *Molecules* **2018**, *23*, 2099.
- (30) Winter, J.; Bevan, S.; Campbell, E. A. Capsaicin and Pain Mechanisms. *Br. J. Anaesth.* **1995**, *75*, 157–168.
- (31) Chakraborty, S.; Adhikary, A.; Mazumdar, M.; Mukherjee, S.; Bhattacharjee, P.; Guha, D.; Choudhuri, T.; Chattopadhyay, S.; Sa, G.; Sen, A.; Das, T. Capsaicin-Induced Activation of PS3-SMAR1 Auto-Regulatory Loop Down-Regulates VEGF in Non-Small Cell Lung Cancer to Restrain Angiogenesis. *PLoS One* **2014**, *9*, No. e99743.
- (32) Clark, R.; Lee, S. H. Anticancer Properties of Capsaicin against Human Cancer. *Anticancer Res.* **2016**, *36*, 837–843.
- (33) Zhang, S.; Wang, D.; Huang, J.; Hu, Y.; Xu, Y. Application of Capsaicin as a Potential New Therapeutic Drug in Human Cancers. *J. Clin. Pharm. Ther.* **2020**, *45*, 16–28.
- (34) Mohammadi-Khanaposhtani, M.; Safavi, M.; Sabourian, R.; Mahdavi, M.; Pordeli, M.; Saeedi, M.; Ardestani, S. K.; Foroumadi, A.; Shafiee, A.; Akbarzadeh, T. Design, Synthesis, in Vitro Cytotoxic Activity Evaluation, and Apoptosis-Induction Study of New 9(10H)-Acridinone-1,2,3-Triazoles. *Mol. Diversity* **2015**, *19*, 787–795.
- (35) Karan, S.; Kashyap, V. K.; Shafi, S.; Saxena, A. K. Structural and Inhibition Analysis of Novel Sulfur-Rich 2-Mercaptobenzothiazole and 1,2,3-Triazole Ligands against *Mycobacterium Tuberculosis DprE1* Enzyme. *J. Mol. Model.* **2017**, *23*, 241.
- (36) Naaz, F.; Preeti Pallavi, M. C.; Shafi, S.; Mulakayala, N.; Shahar Yar, M.; Sampath Kumar, H. M. 1,2,3-Triazole Tethered Indole-3-Glyoxamide Derivatives as Multiple Inhibitors of 5-LOX, COX-2 & Tubulin: Their Anti-Proliferative & Anti-Inflammatory Activity. *Bioorg. Chem.* **2018**, *81*, 1–20.
- (37) Arora, B. S.; Shafi, S.; Singh, S.; Ismail, T.; Kumar, H. M. S. A Novel Domino-Click Approach for the Synthesis of Sugar Based Unsymmetrical Bis-1,2,3-Triazoles. *Carbohydr. Res.* **2008**, *343*, 139–144.
- (38) Ismail, T.; Shafi, S.; Hyder, I.; Sidiq, T.; Khajuria, A.; Alam, S. M.; Halmuthur, M. S. K. Design and Synthesis of Novel 1,2,3-Triazole- and 2-Isoxazoline-Based Bis-Heterocycles as Immune Potentiators. *Arch. Pharm. (Weinheim)* **2015**, *348*, 796–807.
- (39) Haider, S.; Alam, M. S.; Hamid, H.; Shafi, S.; Nargotra, A.; Mahajan, P.; Nazreen, S.; Kalle, A. M.; Kharbanda, C.; Ali, Y.; Alam, A.; Panda, A. K. Synthesis of Novel 1,2,3-Triazole Based Benzoxazinones: Their TNF- α Based Molecular Docking with in-vivo Anti-Inflammatory, Antinociceptive Activities and Ulcerogenic Risk Evaluation. *Eur. J. Med. Chem.* **2013**, *70*, 579–588.
- (40) Lu, H.; Zhou, Q.; He, J.; Jiang, Z.; Peng, C.; Tong, R.; Shi, J. Recent Advances in the Development of Protein–Protein Interactions Modulators: Mechanisms and Clinical Trials. *Signal Transduction Targeted Ther.* **2020**, *5*, 213.
- (41) Nehra, N.; Tittal, R. K.; Ghule, V. D. 1,2,3-Triazoles of 8-Hydroxyquinoline and HBT: Synthesis and Studies (DNA Binding, Antimicrobial, Molecular Docking, ADME, and DFT). *ACS Omega* **2021**, *6*, 27089–27100.
- (42) Agouram, N.; El Hadrami, E. M.; Bentama, A. 1,2,3-Triazoles as Biomimetics in Peptide Science. *Molecules* **2021**, *26*, 2937.
- (43) Bozorov, K.; Zhao, J.; Aisa, H. A. 1,2,3-Triazole-Containing Hybrids as Leads in Medicinal Chemistry: A Recent Overview. *Bioorg. Med. Chem.* **2019**, *27*, 3511–3531.
- (44) Bonandi, E.; Christodoulou, M. S.; Fumagalli, G.; Perdicchia, D.; Rastelli, G.; Passarella, D. The 1,2,3-Triazole Ring as a Bioisostere in Medicinal Chemistry. *Drug Discovery Today* **2017**, *22*, 1572–1581.
- (45) Sahu, A.; Sahu, P.; Agrawal, R. A Recent Review on Drug Modification Using 1,2,3-Triazole. *Curr. Chem. Biol.* **2020**, *14*, 71–87.
- (46) Wei, G.; Luan, W.; Wang, S.; Cui, S.; Li, F.; Liu, Y.; Liu, Y.; Cheng, M. A Library of 1,2,3-Triazole-Substituted Oleanolic Acid Derivatives as Anticancer Agents: Design, Synthesis, and Biological Evaluation. *Org. Biomol. Chem.* **2015**, *13*, 1507–1514.
- (47) Liang, T.; Sun, X.; Li, W.; Hou, G.; Gao, F. 1,2,3-Triazole-Containing Compounds as Anti-Lung Cancer Agents: Current Developments, Mechanisms of Action, and Structure–Activity

Relationship. *Front. Pharmacol.* **2021**, *12*, DOI: 10.3389/fphar.2021.661173.

(48) Chandrashekhar, M.; Nayak, V. L.; Ramakrishna, S.; Mallavadhani, U. V. Novel Triazole Hybrids of Myrrhanone C, a Natural Polygodane Triterpene: Synthesis, Cytotoxic Activity and Cell Based Studies. *Eur. J. Med. Chem.* **2016**, *114*, 293–307.

(49) Nerella, S.; Kankala, S.; Gavaji, B. Synthesis of Podophyllotoxin-Glycosyl Triazoles via Click Protocol Mediated by Silver (I)-N-Heterocyclic Carbenes and Their Anticancer Evaluation as Topoisomerase-II Inhibitors. *Nat. Prod. Res.* **2021**, *35*, 9–16.

(50) Goud, N. S.; Pooladanda, V.; Mahammad, G. S.; Jakkula, P.; Gatreddi, S.; Qureshi, I. A.; Alvala, R.; Godugu, C.; Alvala, M. Synthesis and Biological Evaluation of Morpholines Linked Coumarin-Triazole Hybrids as Anticancer Agents. *Chem. Biol. Drug Des.* **2019**, *94*, 1919–1929.

(51) Seghetti, F.; Di Martino, R. M. C.; Catanzaro, E.; Bisi, A.; Gobbi, S.; Rampa, A.; Canonico, B.; Montanari, M.; Krysko, D. V.; Papa, S.; Fimognari, C.; Belluti, F. Curcumin-1,2,3-Triazole Conjugation for Targeting the Cancer Apoptosis Machinery. *Molecules* **2020**, *25*, 3066.

(52) Lin, S.-Y.; Chang Hsu, Y.; Peng, Y.-H.; Ke, Y.-Y.; Lin, W.-H.; Sun, H.-Y.; Shiao, H.-Y.; Kuo, F.-M.; Chen, P.-Y.; Lien, T.-W.; Chen, C.-H.; Chu, C.-Y.; Wang, S.-Y.; Yeh, K.-C.; Chen, C.-P.; Hsu, T.-A.; Wu, S.-Y.; Yeh, T.-K.; Chen, C.-T.; Hsieh, H.-P. Discovery of a Furanopyrimidine-Based Epidermal Growth Factor Receptor Inhibitor (DBPR112) as a Clinical Candidate for the Treatment of Non-Small Cell Lung Cancer. *J. Med. Chem.* **2019**, *62*, 10108–10123.

(53) Han, C.; Huang, Z.; Zheng, C.; Wan, L.; Zhang, L.; Peng, S.; Ding, K.; Ji, H.; Tian, J.; Zhang, Y. Novel Hybrids of (Phenylsulfonyl)Furoxan and Anilinopyrimidine as Potent and Selective Epidermal Growth Factor Receptor Inhibitors for Intervention of Non-Small-Cell Lung Cancer. *J. Med. Chem.* **2013**, *56*, 4738–4748.

(54) Siudem, P.; Paradowska, K.; Bukowicki, J. Conformational Analysis of Capsaicin Using ¹³C, ¹⁵N MAS NMR, GIAO DFT and GA Calculations. *J. Mol. Struct.* **2017**, *1146*, 773–781.

(55) Sharma, V.; Qayum, A.; Kaul, S.; Singh, A.; Kapoor, K. K.; Mukherjee, D.; Singh, S. K.; Dhar, M. K. Carbohydrate Modifications of Neoandrographolide for Improved Reactive Oxygen Species-Mediated Apoptosis through Mitochondrial Pathway in Colon Cancer. *ACS Omega* **2019**, *4*, 20435–20442.

(56) Kim, S. K.; Im, G. J.; An, Y. S.; Lee, S. H.; Jung, H. H.; Park, S. Y. The Effects of the Antioxidant α -Tocopherol Succinate on Cisplatin-Induced Ototoxicity in HEI-OC1 Auditory Cells. *Int. J. Pediatr. Otorhinolaryngol.* **2016**, *86*, 9–14.

(57) Dheer, D.; Behera, C.; Singh, D.; Abdullaha, M.; Chashoo, G.; Bharate, S. B.; Gupta, P. N.; Shankar, R. Design, Synthesis and Comparative Analysis of Triphenyl-1,2,3-Triazoles as Anti-Proliferative Agents. *Eur. J. Med. Chem.* **2020**, *207*, No. 112813.

(58) Kang, Y.-H.; Lee, E.; Choi, M.-K.; Ku, J.-L.; Kim, S. H.; Park, Y.-G.; Lim, S.-J. Role of Reactive Oxygen Species in the Induction of Apoptosis by α -Tocopheryl Succinate. *Int. J. Cancer* **2004**, *112*, 385–392.

(59) Kumar, A.; Singh, B.; Mahajan, G.; Sharma, P. R.; Bharate, S. B.; Minto, M. J.; Mondhe, D. M. A Novel Colchicine-Based Microtubule Inhibitor Exhibits Potent Antitumor Activity by Inducing Mitochondrial Mediated Apoptosis in MIA PaCa-2 Pancreatic Cancer Cells. *Tumor Biol.* **2016**, *37*, 13121–13136.